University of Alberta

RATE ADAPTIVE TRANSMISSION IN COOPERATIVE NETWORKS

by

Prasanna Kalansuriya

A thesis submitted to the Faculty of Graduate Studies and Research in partial fulfillment of the requirements for the degree of

Master of Science

in

Communications

Department of Electrical and Computer Engineering

Examining Committee

Dr. Chintha Tellambura, Electrical Engineering

Dr. Masoud Ardakani, Electrical Engineering

Dr. Ehab Elmallah, Computing Science

To my parents

Abstract

Cooperative wireless communication uses relays to enhance the capacity and reliability of data transmission. Adaptive transmission is typically used in conventional non-cooperative communications to exploit the time-varying nature of the wireless channel. In this thesis, we combine these two techniques. We consider decode-and-forward (DF) and amplify-and-forward (AF) relays. The wireless environment is modeled by using the Nakagami-m distribution. The achievable channel capacity with rate adaptive transmission is analytically derived for DF and AF cooperative networks. The performance of a DF cooperative network is analyzed with a constant power rate adaptive scheme consisting of a discrete set of transmission modes. The effect of decoding errors on DF cooperative networks is also analyzed. To this end, a new heuristic approximation of the total received signal-to-noise ratio at the destination is developed. This approximation enables simple yet accurate performance analysis.

Acknowledgements

I would like to extend my sincere thanks to my supervisor, Dr. Chintha Tellambura, for his support and supervision. His continuous advice, guidance and encouragement have been instrumental in making this work a success. It has been a great privilege to be a part of his research team.

I also wish to thank the members of my thesis committee, Dr. Masoud Ardakani and Dr. Ehab Elmallah, for their valuable comments and advice in improving this thesis.

Many thanks my colleagues and friends at the iCORE communications laboratory for their help and support in various aspects of my research. It has been a pleasure working with them, and I enjoy their company.

My sincere appreciation and gratitude go to my family for their constant love, support and encouragement throughout my stay in Edmonton.

Table of Contents

List of Tables

List of Figures

List of Symbols

arg	Argument
$\mathbf{Z}^+$	Set of positive integers
$\mathbf{E}\{X\}$	Statistical average of random variable X
$M_X(s)$	Moment generating function of random variable X
$f_X(x)$	Probability density function of random variable X
Pr	Probability
$_2F_1$	Gauss hypergeometric function
$\Gamma(x)$	Gamma function
$\Gamma(a, x)$	Upper incomplete gamma function
$\gamma(a, x)$	Lower incomplete gamma function
$x\,!$	Factorial
$\binom{N}{k}$	Combinations of k elements from N elements
erfc^{-1}	Inverse error function
$Q(x)$	Standard Gaussian Q-function

Acronyms

AF Amplify-and-Forward

AMQAM Adaptive M-ary Quadrature Modulation

AWGN Additive White Gaussian Noise

BER bit error rate

BFSK Binary Frequency Shift Keying

BPSK Binary Phase Shift Keying

C-MRC Cooperative Maximal Ratio Combining

CSI Channel State Information

DF Decode-and-Forward

EGPRS Enhanced General Packet Radio Service

i.i.d. Independent and identically distributed

MGF Moment Generating Function

MIMO Multiple Input Multiple Output

MISO Multiple Input Single Output

ML Maximum Likelihood

M-QAM M-ary Quadrature Amplitude Modulation

MRC Maximal Ratio Combining

MSP Mode Selection Probability

OFDM Orthogonal Frequency Division Multiplexing

ORA Optimal Rate Adaptation

PDF Probability Density Function

PL Piece wise Linear

QAM Quadrature Amplitude Modulation

QoS Quality of Service

QPSK Quadrature Phase Shift Keying

RF Radio Frequency

SNR Signal to Noise Ratio

WAVE Wireless Access for Vehicular Environments

WCDMA Wideband Code Division Multiple Access

WIMAX Worldwide Interoperability for Microwave Access

WLAN Wireless Local Area Network

Chapter 1

Introduction

1.1 Motivation

Consumer demand for low-cost, high-speed, high-quality mobile content delivery has fueled a phenomenal growth in the wireless communication industry during the past few decades. New wireless technologies and standards have emerged to satisfy the ever-increasing demand for mobile and wireless connectivity. Novel methods and improvements of existing techniques are continually being developed to squeeze in more information bits through the wireless channel [1–3].

The wireless channel can rapidly fluctuate and presents a fundamental challenge for reliable data communication. Transmit signals are being distorted by fading due to multipath propagation and by shadowing due to large obstacles in the signal path [4]. Diversity techniques can mitigate these distortions and enhance the capacity and reliability of communication. Techniques such as Orthogonal Frequency Division Multiplexing (OFDM) uses frequency diversity [5] whereas Multiple Input Multiple Output (MIMO) [6] antenna systems uses spatial diversity to achieve high-capacity and reliable communication.

Adaptive transmission techniques can exploit the time-varying nature of the wireless channel. The key idea is to adjust communication parameters according to the channel conditions. IEEE standards 802.11 and 802.16, which are used in wireless technologies such as WLAN, WIMAX and WAVE, use these techniques for reliable, high-speed communication under mobile and ad-hoc wireless

networks [7–9].

Moreover, subscriber handsets are increasingly being miniaturized. Diversity techniques such as MIMO requiring the use of multiple antennae are difficult to implement on small handsets. As a result, the concept of **cooperative diversity** [10] has gained much attention as an alternative approach to creating virtual multiple antenna networks through the cooperation of multiple devices. Extensive research has been performed on using different protocols, network topologies and techniques for achieving cooperative diversity. However, the case of adaptive transmission with cooperative networks has been investigated only recently [11–15]. Motivated by these observations, this thesis focuses on the integration of cooperative diversity networks and rate adaptive transmission.

1.2 Cooperative Diversity

As mentioned before, a wireless communication channel is inherently susceptible to deep signal fades caused by the multipath propagation of radio frequency (RF) signals. The constructive and destructive addition of multipath signals arriving at the receiver results in rapid fluctuation of the received signal. The typical bit error performance of such a fading wireless link is inversely proportional to the total received signal-to-noise ratio (SNR) [16]. The bit error rate (BER) in this case decays slowly as the SNR is increased. Although the BER can be reduced by increasing the transmit signal power, this solution is inefficient and costly. A better solution is to use several independent wireless links between the transmitter and the receiver. This method results in a significant reduction in the BER since the probability of simultaneous deep fades in multiple links is small. If the average BER performance resulting in the use of L independent (diverse) links is inversely proportional to γ^m, where γ is the received SNR, then $m \ (\leq L)$ is called the **diversity order**. The system is said to achieve **full diversity order** when $m = L$. The technique of using multiple links is commonly called diversity. Independent links may be created in time, frequency and space, leading to time diversity, frequency diversity and spatial diversity, respectively.

References [10,17] proposed cooperative diversity. A basic cooperative network (Fig. 1.1) consists of a source, relays or cooperative nodes and a destination. Source transmission intended for a particular destination is overheard by other devices due to the broadcast nature of the channel. These devices play the role of relaying stations and forward the received signal to the destination. The spatial separation among the cooperative relays and the source creates multiple independent links between the source and the destination. In addition to the better error performance resulting from diversity benefits, cooperation results in greater coverage and low power consumption for the transmitting stations [18]. The cooperation among a set of distinct single antenna devices creates a virtual MIMO network.

Although the concept of cooperative diversity appears to be recent, relays have always been used in many applications simply as a tool for extending the reach of a communication network. Relaying stations are commonly used in cellular networks [19–21], for example, to improve the quality of signal reception at blind spots in the network, to provide indoor coverage inside buildings where the line-of-sight or the scattered reception of RF signals is very low, and so on. The basic communication channel involving a relaying station was initially investigated in [22] where the capacity of a three-node network comprised of a source, relay and destination was analyzed under additive white Gaussian noise (AWGN). However, in cooperative communication, the role of the relaying station is dynamic and not fixed as in [22], with users mutually helping each other in relaying information when required. Also, cooperative communication deals with wireless channels under fading and shadowing where cooperation would allow diversity benefits. Apart from these differences, many of the concepts used in the research of cooperative networks were first detailed in [22].

Relaying is pivotal in the operation of a cooperative network. Relaying stations can be user nodes or dedicated fixed terminals. When the user nodes of the network serve as relays, those nodes must send both their own information and that of other nodes. To ensure efficient operation in such a situation, a balance is required between sending the user nodes' own data and the cooperative data [23, 24]. On the

other hand, terminals serving as dedicated relays can simply focus on assisting the transmission of other nodes. Relays can operate as full duplex or half duplex depending on whether they transmit and receive signals at the same time [25]. The full duplex operation is achieved through the use of two frequency bands for transmitting and receiving (Frequency Division Duplexing, FDD), which is a viable option for infrastructure-based dedicated relays [26]. For user node relays, half duplex operation is more suitable where two time slots can be used for the reception and transmission (Time Division Duplexing, TDD).

Among the many protocols in the literature [10], two prominent methods of relaying information are (1) Amplify-and-Forward (AF) and (2) Decode-and-Forward (DF). In the AF method, Fig. 1.1 (a), the relay simply amplifies and forwards the received signal of the source towards the intended destination. No other processing of the received signal is done at the relay. When the destination uses a suitable algorithm such as maximal ratio combining (MRC) to combine the direct signal from the source and the relayed signals, full diversity is realized. Even though the simplicity of the AF scheme makes it an attractive method of cooperation, direct amplifying and forwarding signals require RF hardware. Hence, this type of relaying may be more suited for infrastructure based relays, which permanently serve as relaying stations.

A DF relay, Fig. 1.1 (b), performs demodulation and detection of the received signal and forwards a freshly encoded and modulated signal to the intended destination. This type of relaying can be implemented by using digital signal processing, where provisions are available for storing the received source signal before processing and retransmission.

1.3 Adaptive Transmission

A traditional approach to combating fading is to set aside a fade margin or (in other words) use higher transmission power so that the received SNR remains, at a high probability, above a certain threshold value. This approach not only reduces the power efficiency, but also increases the interference to other users sharing the same
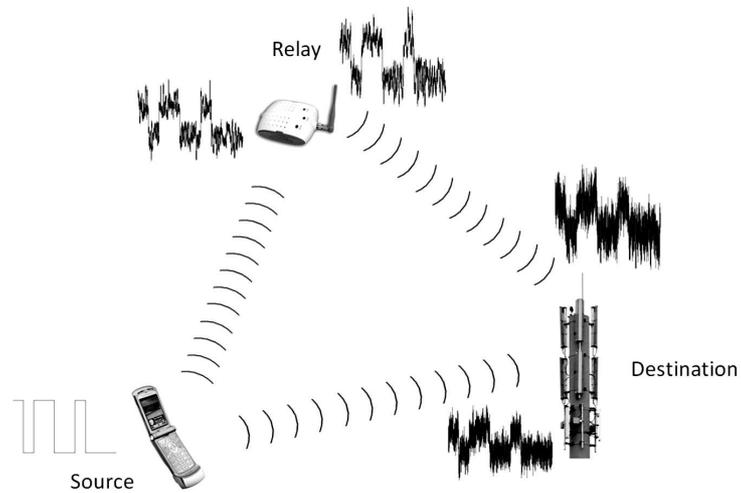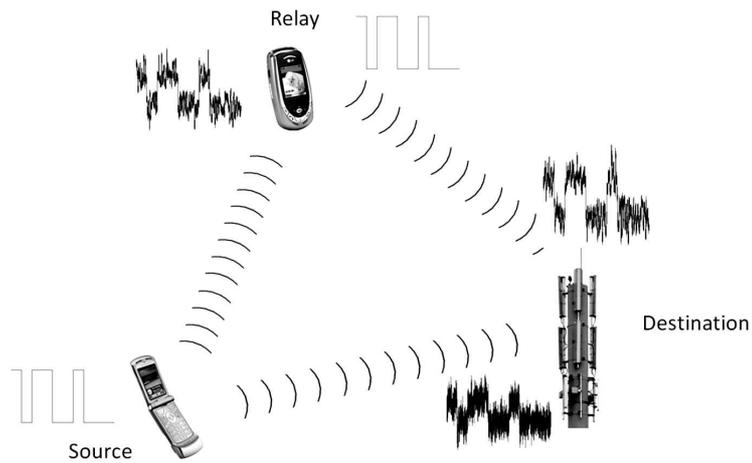
Figure 1.1: (a) Amplify-and-forward cooperative network (b) Decode-and-Forward cooperative network

wireless channel. The fade margins required for wireless mobile channels can be as high as 30 dB. These margins are undesirable for mobile nodes with limited battery power.

Adaptive transmission [4] introduces a paradigm shift by seeking to mitigate or (in certain cases) exploit time variation of the received signal strength. De-

pending on the requirements, the system can achieve guaranteed error rates, higher throughput/spectral efficiency, reduced average transmission power, and other benefits. Transmitter parameters such as transmission power, modulation scheme, constellation size, and coding techniques are adaptively changed based on the channel conditions and user requirements. Thus, adaptation requires the transmitter to know the instantaneous channel conditions. Although adaptation is not effective for fast-fading channels, it is applicable for most slow-fading scenarios in both narrowband and wideband systems. Wideband systems (e.g., systems based on spread spectrum or ultra-wideband technology) should also take measures to combat frequency selective fading. Although the concept of adaptive transmission goes back to the 1960s [27, 28], it was not technically feasible, and not much research was done on optimum adaptive schemes for wireless communication until the 1990s [29, 30]. The keen interest in adaptive transmission may also be attributed to the ever-growing need to exploit more effectively the scarce spectral resources. As a result, all standards for cellular systems (e.g., EGPRS, WCDMA), broadband wireless networks (e.g., WIMAX), local area networks (IEEE 802.11 series), and so on utilize some form of adaptive transmission [31–33].
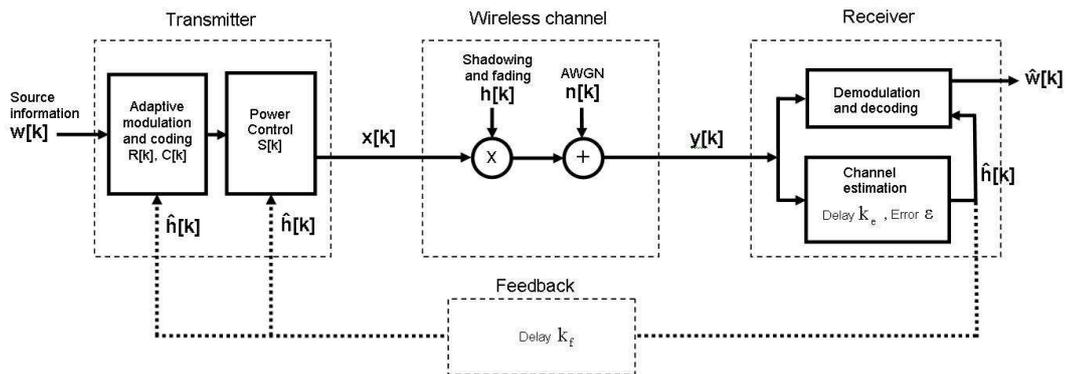
Figure 1.2: System model for an adaptive transmitter and receiver

An adaptive system (Fig. 1.2) is comprised of a transmitter capable of adjusting transmission parameters, the communication channel (which is influenced by the effects of multipath fading, shadowing and noise), a receiver capable of demodu-

6

lation and detection under adaptation and estimation of channel state information (CSI), and a reliable feedback path for sending CSI from the receiver to the transmitter. The rate of adaptation is constrained by the feedback overhead as well as the time delay. Hence, adaptation is performed on a symbol-by-symbol basis, or more practically, on a frame-by-frame basis. Thus, only the slow-fading component can be exploited/combated by adaptation [34]; immunity to fast fading should be obtained by having a fixed fade margin. This margin is significantly smaller than that without adaptation, justifying the complexity of practical adaptation schemes.

As mentioned before, adaptive systems seek to optimize a QoS criterion (e.g., average throughput, bit error rate (BER), delay, information-outage probability, and others) by varying one or more transmission parameters according to the CSI available at the transmitter. Consider Fig. 1.2, where a discrete time model based on symbol duration T_s is used. Symbols $w[k]$ denote the source information bits arriving at the transmitter, which are coded and modulated as $x[k]$, for the k-th channel-use. The wireless channel is modeled by the channel coefficient $h[k]$, which may include the effects of path loss, shadowing and multi-path fading. The additive noise term $n[k]$ is assumed to be Gaussian. The receiver estimates the channel coefficient to be $\hat{h}[k]$ with a certain delay k_e and an error ϵ. The estimate is used for demodulation and detection of the received signal and is also fed back reliably to the transmitter, with another delay k_f. This information is used to adapt the transmit power $S[k]$, the transmission rate $R[k]$ and/or the transmission coding scheme $C[k]$. Further analysis of this model is found in [4, 35, 36]. The model is accurate when the total delay $(k_e + k_f)$ is smaller than the coherence time of the wireless channel.

In transmission rate adaptation, the transmitter adjusts and varies its data rate, i.e., the number of information bits transmitted per unit of time, to achieve the required QoS. For instance, consider a scheme which adapts the transmission rate to satisfy the QoS constraint of the maximum allowable BER. A transmitter based on this scheme could use higher bit rates (i.e., higher numbers of bits in each symbol or frame) when channel conditions are favorable, and lower bit rates otherwise. Such a

scheme may be implementable in two ways: either by varying the symbol duration or by changing the constellation size (of the modulation scheme). The former is not easily implementable as corresponding variation of the signal bandwidth makes effective bandwidth sharing more complicated [4]. Therefore, practical systems vary the constellation size.

Transmission power adaptation involves changing the transmit signal power according to the CSI. **Water-filling** in time and **channel inversion** are two commonly used techniques for power adaptation [4]. In the water-filling technique, originally proposed in [35], more power is allocated to time instances where the channel is favorable with respect to a threshold level (the water level). Water-filling maximizes the ergodic capacity, while accepting a certain probability of outage, but benefits of water-filling can be reaped only by adapting the modulation scheme accordingly. On the other hand, channel inversion tries to maintain a constant received SNR by inverting the effects of channel fading.

Channel coding is used to protect the information transmitted against the detriments of the wireless channels. Adaptive coding adjusts the strength of the coding scheme used according to the prevailing channel conditions; stronger low rate codes are used under bad channel conditions, and weaker higher rate codes are employed under favorable conditions [4].

The adaptive techniques discussed so far can also be used in combination to enhance their effectiveness. That is, multiple transmission parameters can be simultaneously varied to make the system adapt to the channel conditions. Reference [35] presents an analysis of one such scheme, where the transmission power and transmission rate are varied simultaneously to maximize spectral efficiency while meeting a BER constraint.

1.4   Contributions

The main focus of this thesis is the performance of DF cooperative networks with rate adaptive transmission. The channel capacity, average BER, probability of outage and average spectral efficiency are analyzed. The DF results are compared with

those of AF cooperative networks.

First, the achievable channel capacity under rate adaptive transmission for a DF cooperative network is derived. The capacity of a cooperative network with adaptive transmission was initially investigated in [11]. Reference [13] extends the work of [11] to a multiple parallel cooperative relay network. We generalize the work of [11, 13] by focusing on DF cooperation, and the wireless environment involved in the analysis is more generalized to Nakagami-m fading. This work was presented at in the IEEE CCECE conference in May 2009 [37].

Next, a rate-adaptive scheme with a discrete set of transmission modes using M-ary quadrature amplitude modulation (M-QAM) is considered. Two types of rate adaptation schemes are analyzed: (1) rate adaptation using fixed switching thresholds and (2) rate adaptation using optimized switching thresholds. The system performance under both schemes is derived by using metrics such as the BER, outage probability and average throughput. Here, we extend the the results of [15] where an AF cooperative network was analyzed under the Rayleigh fading model, to a DF cooperative network over Nakagami-m fading. The results of this work will appear in the proceedings of the IEEE ICC conference held in June 2009 [38].

Finally, the use of cooperative demodulation and cooperative diversity combining techniques for DF cooperative networks is investigated. A heuristic approximation for the total received SNR at the destination is proposed for DF cooperation under the cooperative MRC (C-MRC) scheme. The performance under this scheme is derived. This work is submitted to the IEEE Transactions on Wireless Communications and is currently under review [39].

1.5   Outline of thesis

This chapter briefly discussed cooperative networks and rate adaptation. The concepts of diversity, cooperative diversity, cooperative networks and adaptive transmission were presented.

Chapter 2 presents the overall system and channel models used throughout the thesis. The theoretical achievable channel capacity for rate adaptive transmission

and cooperative networks is found. Both DF and AF cooperative networks are considered.

In Chapter 3, the performance of a cooperative DF relay network is investigated under adaptive M-QAM. Rate adaptive transmission is achieved through the use of a discrete set of M-QAM constellations. Two types of rate adaptation are considered: one using fixed switching levels and the other using optimized switching levels. Outage probability, mode selection probability, average BER, and average spectral efficiency are used in the evaluation of the system performance.

Cooperative diversity combining, demodulation and detection techniques are discussed in Chapter 4. The effect of decoding errors at the relays on the overall system performance is investigated. The cooperative diversity combining technique of C-MRC is used for this purpose with discrete rate adaptive transmission. A heuristic approximation for the total received SNR is used in the performance analysis.

Finally, Chapter 5 presents our conclusions and suggests some potential future research initiatives resulting from this work.

Chapter 2

Capacity of a Cooperative Network under Rate Adaptive Transmission

2.1 Introduction

Rate adaptive transmission exploits the variation of the channel gain to vary the transmission rate while cooperative diversity uses relays to enhance the wireless network performance. In this chapter, we analyze a wireless system which incorporates both of these techniques[1].

The theoretical limits of the capacity of DF cooperative networks under rate adaptive transmission is investigated. For the simplicity of the analysis, we assume error-free symbol decoding at the cooperative relays. The results are also compared to those of a comparable AF cooperative network. A general wireless channel model, Nakagami-m fading, is used to model the wireless environment under both independent and identically distributed (i.i.d.) and non-i.i.d. fading conditions.

The rest of the chapter is organized as follows. Section 2.2 describes the wireless channel model used in the analysis. The system models of the AF and DF cooperative networks are detailed in Section 2.3. The mathematical derivations of the channel capacity are detailed in Section 2.4. Finally, Section 2.5 discusses the simulation and numerical results.

---

[1]A version of this chapter has been presented at the IEEE Canadian Conference on Electrical and Computer Engineering (CCECE) 2009 held in St. John's, Newfoundland, Canada [37].

2.2 Wireless Channel Model

Throughout this thesis, the wireless multipath fading environment between any two wireless nodes is modeled by using the Nakagami-m fading model [40]. This model is flexible enough to describe various fading environments by the correct choice of its parameters and can model a wide range of fading conditions ranging from line-of-sight to non-line-of-sight, Rayleigh fading, and one-sided Gaussian fading. Importantly, the Nakagami-m fading model provides a good match for urban and indoor multipath propagation [41,42]. With this model, the envelope of the received signal α is described by the probability density function (PDF) [43]

$$f_\alpha(\alpha) = \frac{2m^m \alpha^{2m-1}}{\Omega^m \Gamma(m)} \exp\left(-\frac{m\alpha^2}{\Omega}\right) \qquad \alpha \geq 0, \quad m \geq 0.5\,, \qquad (2.1)$$

where m is the shape parameter, and Ω is the average power of the received envelope. The phase ϕ of the received signal is assumed to be uniformly distributed over $[0, 2\pi]$. For ideal coherent phase detection, the receiver compensates for ϕ, and only the envelope fading distribution (2.1) is required for our analysis. The resulting SNR γ is Gamma distributed with shape parameter m and scale parameter $\bar{\gamma}/m$, with the PDF [43]

$$f_\gamma(\gamma) = \frac{m^m \gamma^{m-1}}{\bar{\gamma}^m \Gamma(m)} \exp\left(-\frac{m\gamma}{\bar{\gamma}}\right) \qquad \gamma \geq 0\,, \qquad (2.2)$$

where $\overline{\gamma}$ is the average received SNR which is equal to $\Omega E_s/N_0$, E_s is the transmit symbol energy, and N_0 is the one-sided power spectral density of AWGN.

The delay spread and the Doppler spread of the wireless channel largely determine its dynamic and varying nature. The delay spread gives the time dispersion of the signals arriving from different paths. The rate at which the wireless channel changes is determined by the Doppler spread, which is governed by the relative motion between the transmitter and the receiver. We assume that the wireless channel varies slowly and that flat fading occurs; i.e., that the delay spread and Doppler spread are low [44]. Under this assumption, the wireless channel changes at a rate much slower than the symbol rate of transmission [34]. For an example, a Doppler spread of 20 Hz and a symbol rate of 1×10^6 per second make the channel remain stable over several $10,000$ symbol intervals.
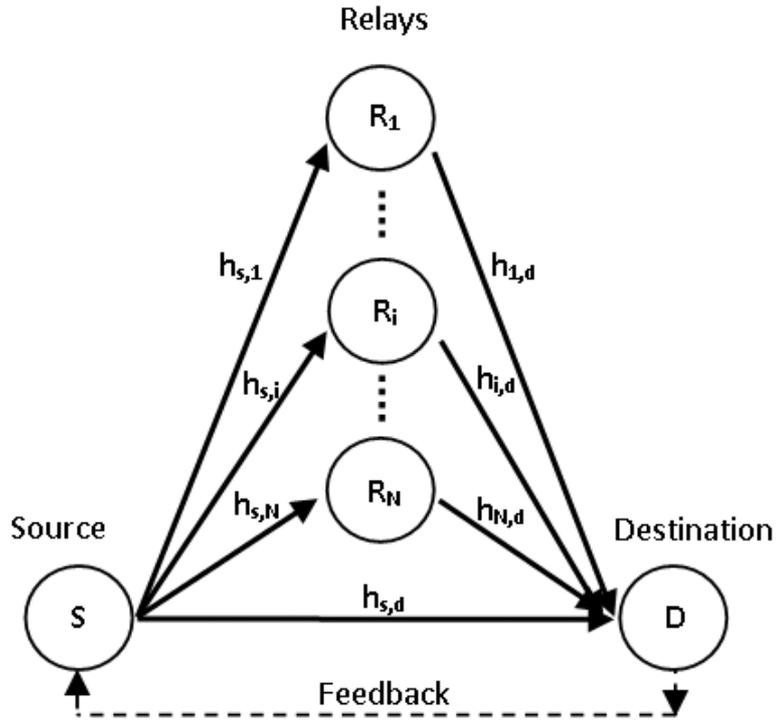
Figure 2.1: Relay network with adaptive transmission.

2.3   System model of Cooperative Network

The system model of the cooperative network formed by a source node S, destination node D and cooperative relay nodes R_i , $i \in \{1, 2, ..., N\}$ is illustrated in Fig. 2.1. The signal transmission from the source to the destination is assisted by $N \geq 1$ cooperating parallel relays. The transmission occurs in two phases. During the first phase, the source broadcasts its message to the destination and the N relays. In the second phase, each of the relays either amplifies and forwards or decodes and forwards (depending on whether AF or DF relays are used) the signal received in the first phase. Each relay requires an orthogonal channel to forward its information to the destination where maximal ratio combining (MRC) is used for diversity combining of the received signals.

The channel coefficients between D and S, D and R_i and R_i and S are denoted as $h_{s,i}$, $h_{i,d}$, and $h_{s,d}$ with shape parameters $m_{s,i}$, $m_{i,d}$ and $m_{s,d}$, respectively. The corresponding received instantaneous SNR are given as $\gamma_{s,i} = |h_{s,i}|^2 \bar{\gamma}_{s,i}$, $\gamma_{i,d} =$

$|h_{i,d}|^2 \bar{\gamma}_{i,d}$ and $\gamma_{s,d} = |h_{s,d}|^2 \bar{\gamma}_{s,d}$. Both i.i.d. and non-i.i.d. fading environments are considered in the subsequent analysis under AF and DF cooperative relay networks.

2.3.1 AF Cooperative Network

As mentioned before, in an AF relay the signals are amplified and sent to the destination. The signals received at the destination and at the i-th relay from the source transmission are then given as follows:

$$r_{s,d} = h_{s,d}\sqrt{E_s}\, x + n_{s,d} \qquad \text{and} \tag{2.3}$$

$$r_{s,i} = h_{s,i}\sqrt{E_s}\, x + n_{s,i}\,, \quad i = 1, 2, \ldots, N, \tag{2.4}$$

where x is the transmit symbol with unit energy, and $n_{s,d}$ and $n_{s,i}$ are the AWGN terms at the destination and at the i-th relay. These terms are modeled as AWGN with one-sided power spectral density of N_0. The received signal at the destination from the i-th relay is

$$r_{i,d} = G_i\, h_{i,d}\, r_{s,i} + n_{i,d}\,, \quad i = 1, 2, \ldots, N, \tag{2.5}$$

where $n_{i,d}$ is the noise addition at the destination, and G_i is the ith relay amplifier gain, chosen as, $G_i^2 = E_s/(E_s|h_{s,i}|^2 + N_0)$ [10]. The total received SNR at the destination through MRC is easily found as [10]

$$\gamma_{\text{tot}} = \gamma_{s,d} + \sum_{i=1}^{N} \frac{\gamma_{s,i}\gamma_{i,d}}{\gamma_{s,i} + \gamma_{i,d} + 1}\,. \tag{2.6}$$

The performance analysis of the AF network requires the PDF of the total received SNR γ_{tot} for Nakagami-m fading. The exact PDF is complicated and difficult to use in subsequent performance analysis. Hence, γ_{tot} is approximated by using a fairly accurate upper bound γ_{ub} as [45, 46]

$$\gamma_{\text{tot}} \leq \gamma_{s,d} + \sum_{i=1}^{N} \gamma_i = \gamma_{ub}\,, \tag{2.7}$$

where $\gamma_i = \min(\gamma_{s,i}, \gamma_{i,d})$. This upper bound is known to be accurate and has been used extensively in the analysis of AF relays [12–15, 45–47]. The PDFs of

the upper bound of the received SNR for i.i.d. and non-i.i.d. Nakagami-m fading environments are derived in the Appendix.

2.3.2 DF Cooperative Network

The first phase here is identical to that of the AF cooperative network, and the received signals are again described by Eqs. (2.3) and (2.4). However, during the second phase, each relay forwards a signal which is derived from decoding the original signal received from the source. The received signal at the destination during this phase is then given as

$$r_{i,d} = h_{i,d}\sqrt{E_s}\,\hat{x} + n_{i,d}\,, \quad i = 1, 2, \ldots, N, \tag{2.8}$$

where $\hat{x}$ is the decoded and modulated symbol of x. An adaptive DF relaying scheme similar to [10, 48, 49] is used in the model of the DF cooperative network. In this model, it is assumed that a DF relay is able to accurately decode the received signal from the source, without outage, only if the instantaneous received SNR is above a particular threshold value γ_T; i.e., $\gamma_{s,i} > \gamma_T$. γ_T corresponds to the target information rate of R below which outage occurs. This correspondence implies that $\gamma_T = 2^{R(N+1)} - 1$ according to Shannon's channel capacity bound. For the simplicity of analysis, error-free decoding of the received signal is assumed at the relays. This assumption is, however, relaxed in Chapter 4.

Identically Distributed Fading Environment

Here, all channels between all nodes are Nakagami-m fading with identical fading parameters (i.e., $m_{s,d} = m_{s,i} = m_{i,d} = m$) and the same average received SNR ($\bar{\gamma}_{s,d} = \bar{\gamma}_{s,i} = \bar{\gamma}_{i,d} = \bar{\gamma}$). This case may arise when the source, destination and the relays are physically located at equal distances from each other.

Under the adaptive DF scheme, the number of relays forwarding the source message to the destination is a binomial random variable Y, where $Y = \{0, 1, \ldots, N\}$. The probability that y relays forward the received signal to the destination is given as

$$\Pr(Y = y) = \binom{N}{y}\left[\frac{\Gamma\!\left(m, \frac{m\gamma_T}{\bar{\gamma}}\right)}{\Gamma(m)}\right]^y \left[\frac{\gamma\!\left(m, \frac{m\gamma_T}{\bar{\gamma}}\right)}{\Gamma(m)}\right]^{N-y}, \tag{2.9}$$

15

where $\Gamma(a, x) = \int_x^\infty t^{a-1} e^{-t} dt$, $\gamma(a, x) = \int_0^a t^{a-1} e^{-t} dt$, and $\Gamma(a) = (a-1)!$, $a \in \mathbf{Z}^+$. The MRC at the destination gives the total received SNR γ_{tot} as

$$\gamma_{\text{tot}} = \sum_{j=1}^{y+1} \gamma_j, \tag{2.10}$$

where γ_j are Gamma random variables with shape parameter $k = m$ and scale parameter $\theta = \frac{\bar{\gamma}}{m}$. The moment generating function (MGF) of γ_{tot} is derived as

$$M_{\gamma_{\text{tot}}}(s \mid y) = \prod_{i=1}^{y+1} M_{\gamma_j}(s) = \left(1 + \frac{\bar{\gamma}}{m} s\right)^{-m(y+1)}, \tag{2.11}$$

where the MGF of random variable Y is defined as $M_Y(s) = \mathbf{E}\{e^{-sY}\}$, $\mathbf{E}\{\cdot\}$ denotes the statistical average over the random variable. The Laplace inversion of (2.11) gives the PDF of γ_{tot} conditional on Y as

$$f_{\gamma_{\text{tot}}}(\gamma \mid y) = \left(\frac{m}{\bar{\gamma}}\right)^{m(y+1)} \frac{\gamma^{m(y+1)-1}}{(m(y+1)-1)!} e^{-\frac{m\gamma}{\bar{\gamma}}}. \tag{2.12}$$

By using the theorem of total probability and Eqs. (2.9) and (2.12), the unconditional PDF of the total received SNR γ_{tot} can be written as

$$f_{\gamma_{\text{tot}}}(\gamma) = \sum_{i=0}^{N} \left(\frac{m}{\bar{\gamma}}\right)^{m(i+1)} \frac{\gamma^{m(i+1)-1}}{(m(i+1)-1)!} e^{-m\gamma/\bar{\gamma}} \binom{N}{i} \left[\frac{\Gamma\left(m, \frac{m\gamma_T}{\bar{\gamma}}\right)}{\Gamma(m)}\right]^i \left[\frac{\gamma\left(m, \frac{m\gamma_T}{\bar{\gamma}}\right)}{\Gamma(m)}\right]^{N-i}. \tag{2.13}$$

Non Identically Distributed Fading Environment

The channel gains are now modeled by using different Nakagami-m distributions. This case may arise when the distances between different nodes are unequal, and signal scatterers may be unevenly distributed spatially. Hence, the total number of relays forwarding the source message to the destination is a random variable having a generalized binomial distribution with distinct probability of success p_i for each relay (This distribution is a generalization of (2.9)).

The system is best described by using a vector of indicator random variables $\underline{\mathbf{b}}_k$ as

$$\underline{\mathbf{b}}_k = (b_N, b_{N-1}, \ldots, b_i, \ldots, b_2, b_1), \ k = 0, 1, \ldots, 2^N - 1$$

$$\text{with} \quad k = 2^{N-1} b_N + 2^{N-2} b_{N-1} + \ldots + 2b_2 + b_1, \tag{2.14}$$

where b_i's are random variables taking values 1 or 0 to indicate whether or not the i-th relay is forwarding the source message to the destination. $\Pr(b_i = 1) = p_i$ and $\Pr(b_i = 0) = 1 - p_i$ where p_i is the probability that the received SNR at R_i is greater than γ_T. If one complete cycle of cooperation in the network is defined as a state of the network, then the DF relays operating in a particular state k can be represented by using the k-th value of the random vector $\underline{\mathbf{b}}_k$. There are 2^N different states. The probability of observing a combination of DF relays described by $\underline{\mathbf{b}}_k$ is given as

$$\Pr(\underline{\mathbf{b}}_k) = \prod_{i=1}^{N} p_i^{b_i} (1 - p_i)^{(1-b_i)} . \qquad (2.15)$$

The number of DF relays forwarding a source signal to the destination is $N(\underline{\mathbf{b}}_k)$.

$$N(\underline{\mathbf{b}}_k) = \sum_{i=1}^{N} b_i . \qquad (2.16)$$

These relayed signals and the direct source-transmitted signal are received at the destination. They are combined by using MRC, so that the total received SNR γ_{tot} is

$$\gamma_{\text{tot}} = \gamma_{s,d} + \sum_{i=1}^{N} b_i \gamma_{i,d} . \qquad (2.17)$$

The probability $p_i = \Pr(b_i = 1) = \Pr(\gamma_{s,i} > \gamma_T)$ can be calculated by using the PDF of $\gamma_{s,i}$ as

$$p_i = \int_{\gamma_T}^{\infty} \frac{m_{s,i}^{m_{s,i}} x^{m_{s,i}-1}}{\bar{\gamma}_{s,i}^{m_{s,i}} \Gamma(m_{s,i})} e^{-\frac{m_{s,i} x}{\bar{\gamma}_{s,i}}} \, dx = \frac{\Gamma\left(m_{s,i}, \frac{m_{s,i} \gamma_T}{\bar{\gamma}_{s,i}}\right)}{\Gamma(m_{s,i})} . \qquad (2.18)$$

Given that the cooperative network is in a state $k \in \{0, 1, \dots, 2^N - 1\}$ having a DF relay combination described by vector $\underline{\mathbf{b}}_k$, the MGF of γ_{tot} conditioned on $\underline{\mathbf{b}}_k$ can be written as

$$M_{\gamma_{tot}}(s \mid \underline{\mathbf{b}}_k) = M_{\gamma_{s,d}}(s) \prod_{i=1, b_i \neq 0}^{N} M_{\gamma_{i,d}}(s) , \qquad (2.19)$$

with $M_{\gamma_{s,d}}(s) = \left(1 + \frac{\bar{\gamma}_{s,d}}{m_{s,d}} s\right)^{-m_{s,d}}$ and $M_{\gamma_{i,d}}(s) = \left(1 + \frac{\bar{\gamma}_{i,d}}{m_{i,d}} s\right)^{-m_{i,d}}$. Hence, we can rewrite (2.19) as

$$M_{\gamma_{tot}}(s \mid \underline{\mathbf{b}}_k) = \left(1 + \frac{\bar{\gamma}_{s,d}}{m_{s,d}} s\right)^{-m_{s,d}} \prod_{i=1, b_i \neq 0}^{N} \left(1 + \frac{\bar{\gamma}_{i,d}}{m_{i,d}} s\right)^{-m_{i,d}} . \qquad (2.20)$$

17

A partial fraction expansion of (2.20) gives

$$M_{\gamma_{tot}}(s \mid \underline{\mathbf{b}}_k) = \sum_{j=1}^{m_{s,d}} \frac{\Delta_j(\underline{\mathbf{b}}_k)}{\left(1 + \frac{\bar{\gamma}_{s,d}}{m_{s,d}}s\right)^j} + \sum_{i=1,b_i \neq 0}^{N} \sum_{j=1}^{m_{i,d}} \frac{\Psi_{i,j}(\underline{\mathbf{b}}_k)}{\left(1 + \frac{\bar{\gamma}_{i,d}}{m_{i,d}}s\right)^j}, \qquad (2.21)$$

where $\Delta_i(\underline{\mathbf{b}}_k)$ is given in (2.22) for $k \neq 0$ with $\Delta_i(\underline{\mathbf{b}}_0) = 0$ for $i \neq m_{s,d}$ and $\Delta_i(\underline{\mathbf{b}}_0) = 1$ for $i = m_{s,d}$. $\Psi_{i,j}(\underline{\mathbf{b}}_k)$ is defined in (2.23) for $k \neq 0$ with $\Psi_{i,j}(\underline{\mathbf{b}}_0) = 0 \; \forall \, i, j \in \mathbf{Z}$.

$$\Delta_i(\underline{\mathbf{b}}_k) = \frac{\left(\frac{\bar{\gamma}_{s,d}}{m_{s,d}}\right)^{(i-m_{s,d})}}{(m_{s,d} - i)!} \frac{\partial^{m_{s,d}-i}}{\partial s^{m_{s,d}-i}} \left[\prod_{j=1,b_j \neq 0}^{N} \left(1 + \frac{\bar{\gamma}_{j,d}}{m_{j,d}}s\right)^{-m_{j,d}} \right]_{s=-\frac{m_{s,d}}{\bar{\gamma}_{s,d}}}. \qquad (2.22)$$

$$\begin{aligned} \Psi_{i,j}(\underline{\mathbf{b}}_k) &= \frac{\left(\frac{\bar{\gamma}_{i,d}}{m_{i,d}}\right)^{(j-m_{i,d})}}{(m_{i,d} - j)!} \frac{\partial^{m_{i,d}-j}}{\partial s^{m_{i,d}-j}} \left[\left(1 + \frac{\bar{\gamma}_{s,d}}{m_{s,d}}s\right)^{-m_{s,d}} \right. \\ &\qquad \times \left. \left[\prod_{l=1,l \neq i,b_l \neq 0}^{N} \left(1 + \frac{\bar{\gamma}_{l,d}}{m_{l,d}}s\right)^{-m_{l,d}} \right] \right]_{s=-\frac{m_{i,d}}{\bar{\gamma}_{i,d}}}. \end{aligned} \qquad (2.23)$$

The Laplace inversion of (2.21) produces the conditional PDF of the total received SNR at the destination conditional on $\underline{\mathbf{b}}_k$, $f_{\gamma_{tot}}(\gamma \mid \underline{\mathbf{b}}_k)$ as

$$\begin{aligned} f_{\gamma_{tot}}(\gamma \mid \underline{\mathbf{b}}_k) &= \sum_{j=1}^{m_{s,d}} \frac{\Delta_j(\underline{\mathbf{b}}_k)}{(j-1)!} \left(\frac{m_{s,d}}{\bar{\gamma}_{s,d}}\right)^j \gamma^{j-1} e^{-\frac{m_{s,d}\gamma}{\bar{\gamma}_{s,d}}} \\ &\quad + \sum_{i=1,b_i \neq 0}^{N} \sum_{j=1}^{m_{i,d}} \frac{\Psi_{i,j}(\underline{\mathbf{b}}_k)}{(j-1)!} \left(\frac{m_{i,d}}{\bar{\gamma}_{i,d}}\right)^j \gamma^{j-1} e^{-\frac{m_{i,d}\gamma}{\bar{\gamma}_{i,d}}}. \end{aligned} \qquad (2.24)$$

By using the theorem of total probability, the PDF of total received SNR γ_{tot} unconditional on $\underline{\mathbf{b}}_k$ can the be written in terms of (2.15) and (2.24) as

$$f_{\gamma_{tot}}(\gamma) = \sum_{k=0}^{2^N-1} f_{\gamma_{tot}}(\gamma \mid \underline{\mathbf{b}}_k) \Pr(\underline{\mathbf{b}}_k). \qquad (2.25)$$

2.4   Capacity Analysis

In this section, we derive the channel capacity for cooperative DF and AF networks under multipath fading and rate adaptive transmission. No exact mathematical formula is derived for the information capacity of a cooperative network [50] as opposed to the Shannon's channel capacity bound for point-to-point communication,

but this capacity analysis under adaptive transmission still provides a useful insight into the performance of adaptive cooperative networks.

2.4.1 Optimal Rate Adaptation with Constant Transmit Power (ORA)

Under this adaptive scheme, the transmit power is maintained constant, but the transmission rate is adjusted in response to the channel conditions. As shown in Fig. 2.1, the CSI estimated at the receiver is fed back to the transmitter. We assume error-free CSI estimates and a reliable and low-delay feedback channel. With these assumptions, ideal CSI is available at the receiver as well as the transmitter. Therefore, the transmitter can evaluate the rate of transmission that can be achieved without loss of information for each channel instant; i.e., when the received SNR under fading is γ, the channel can support an information rate $C_\gamma = B \log_2(1 + \gamma)$ according to Shannon's channel capacity, where B is the bandwidth. If the transmitter is capable of continuous rate adaptation, then it can adapt its transmission rate optimally according to the instantaneous channel capacity C_γ. Doing so will provide an attainable channel capacity of [35, eq. (8)]

$$C = \int_0^\infty B \log_2(1 + \gamma) f_\gamma(\gamma) \, d\gamma \, , \tag{2.26}$$

where $f_\gamma(\gamma)$ is the PDF of the SNR. The capacity achieved through this scheme is the same as the ergodic capacity of a system using a fixed rate under fading. For the cooperative system in Fig. 2.1, (2.26) needs to be slightly modified to encompass the $N + 1$ orthogonal channels [15]:

$$C_{\text{ora}} = \frac{B}{(N + 1) \ln 2} \int_0^\infty \ln(1 + \gamma) f_\gamma(\gamma) \, d\gamma \, , \tag{2.27}$$

where $\ln(x)$ is the natural logarithm of x.

Analysis of an AF Cooperative Network

An upper bound of the achieved capacity can be derived by using the PDF (A.18) with the ORA channel capacity given in (2.27). Eq. (2.28) gives an upper bound on

19

the channel capacity under ORA for the cooperative AF network.

$$C_{\text{ora}} \leq \frac{B(0.5)^{2N(m-1)}\Gamma^N(2m)}{\ln 2(N+1)m^N\Gamma^{2N}(m)}$$
$$\times \left[\sum_{i=1}^{m} \frac{\Delta_i}{(i-1)!} \left(\frac{m}{\bar{\gamma}}\right)^i \mathcal{I}_i\left(\frac{m}{\bar{\gamma}}\right) \right.$$
$$\left. + \sum_{i=1}^{N(2m-1)} \frac{\Psi_i}{(i-1)!} \left(\frac{2m}{\bar{\gamma}}\right)^i \mathcal{I}_i\left(\frac{2m}{\bar{\gamma}}\right) \right]. \qquad (2.28)$$

The integral $\mathcal{I}_n(\mu) = \int_0^\infty t^{n-1}\ln(1+t)e^{-\mu t}dt$, $\mu > 0$; $n \in \mathbf{Z}^+$, can be evaluated in closed-form as in [34, eq.(78)]. Similarly, for the case of non-i.i.d. fading channels the PDF given in (A.42) is used to derive the capacity as

$$C_{\text{ora}} \leq \frac{B}{(N+1)\ln 2} \left[\prod_{i=1}^{N} D_i\right] \left[\sum_{i=1}^{m_{s,d}} \frac{\Delta_i}{(i-1)!} \left(\frac{m_{s,d}}{\bar{\gamma}_{s,d}}\right)^i \mathcal{I}_i\left(\frac{m_{s,d}}{\bar{\gamma}_{s,d}}\right) \right.$$
$$\left. + \sum_{i=1}^{N} \sum_{j=1}^{m_{s,i}+m_{i,d}} \frac{\Psi_{ji}}{(j-1)!} \left(\frac{m_{s,i}\bar{\gamma}_{i,d}+m_{i,d}\bar{\gamma}_{s,i}}{\bar{\gamma}_{s,i}\bar{\gamma}_{i,d}}\right)^j \mathcal{I}_j\left(\frac{m_{s,i}\bar{\gamma}_{i,d}+m_{i,d}\bar{\gamma}_{s,i}}{\bar{\gamma}_{s,i}\bar{\gamma}_{i,d}}\right) \right].$$
$$(2.29)$$

Analysis of DF Cooperative Network

For DF cooperative networks over i.i.d. fading channels and non-i.i.d. fading channels, the PDFs of the received SNR (2.13) and (2.24), respectively, are used to obtain the capacity under ORA by using (2.27). The capacity under the ORA scheme for the i.i.d. case and non-i.i.d. case are given in (2.30) and (2.31), respectively.

$$C_{\text{ora}} = \frac{B}{\ln 2} \sum_{i=0}^{N} \binom{N}{i} \left[\frac{\Gamma\left(m, \frac{m\gamma_T}{\bar{\gamma}}\right)}{\Gamma(m)}\right]^i \left[\frac{\gamma\left(m, \frac{m\gamma_T}{\bar{\gamma}}\right)}{\Gamma(m)}\right]^{N-i}$$
$$\times \left(\frac{m}{\bar{\gamma}}\right)^{m(i+1)} \frac{1}{(i+1)\Gamma(m(i+1))} \mathcal{I}_{m(i+1)}\left(\frac{m}{\bar{\gamma}}\right). \qquad (2.30)$$

$$C_{\text{ora}} = \frac{B}{\ln 2} \sum_{k=0}^{2^N-1} \frac{\Pr(\mathbf{b}_k)}{(1+N(\mathbf{b}_k))} \left[\sum_{j=1}^{m_{s,d}} \frac{\Delta_j(\mathbf{b}_k)}{(j-1)!} \left(\frac{m_{s,d}}{\bar{\gamma}_{s,d}}\right)^j \mathcal{I}_j\left(\frac{m_{s,d}}{\bar{\gamma}_{s,d}}\right) \right.$$
$$\left. + \sum_{i=1,b_i \neq 0}^{N} \sum_{j=1}^{m_{i,d}} \frac{\Psi_{i,j}(\mathbf{b}_k)}{(j-1)!} \left(\frac{m_{i,d}}{\bar{\gamma}_{i,d}}\right)^j \mathcal{I}_j\left(\frac{m_{i,d}}{\bar{\gamma}_{i,d}}\right) \right]. \qquad (2.31)$$

2.5 Observations and Comparisons of Results

In this section, the analytical expressions for the channel capacity are compared with the Monte Carlo simulations. The channel gains are obtained through random variable generation. Each simulation data point for a given average SNR is obtained by using 1×10^6 random values of the channel gain. These values were used in the analytical equations derived in Section 2.4. Here, the integration operation using the PDF of the channel statistics is replaced by taking the algebraic mean or expected value of all the numerical values obtained. This technique amounts to a semi-analytical simulation. Compared to conventional Monte Carlo simulation, this method significantly reduces the size of the sample set and computational cost required to obtain a simulation result of a given accuracy and confidence interval [51]. For example, with a sample set size of 1×10^6 and an average SNR of $10\,\mathrm{dB}$, the simulated capacity for the non-i.i.d. AF relay network lies within the confidence interval $(1.0104, 1.0112)$ with a confidence of 90%.

For the analysis, a cooperative network consisting of two parallel relays is considered for both the AF and DF cases. In the i.i.d. fading case, Nakagami fading parameter is taken as $m = 2$, and in the case of non-i.i.d. fading, the following Nakagami fading parameters and average SNR values are considered: $\bar{\gamma}_{s,d} = 0.5\rho$, $\bar{\gamma}_{s,1} = 0.2\rho$, $\bar{\gamma}_{s,2} = 0.7\rho$, $\bar{\gamma}_{1,d} = 0.9\rho$, $\bar{\gamma}_{2,d} = 0.4\rho$, $m_{s,d} = 2$, $m_{s,1} = 1$, $m_{s,2} = 2$, $m_{1,d} = 3$, $m_{2,d} = 1$, where ρ is the average SNR.

The PDF of the total received SNR γ_{tot} is shown in Fig. 2.3. The decoding threshold γ_T is chosen to be $5\,\mathrm{dB}$, and PDF plots are obtained for different average SNR values near γ_T. A large variation in the shape of PDF's can be seen around $\rho = \gamma_T$.

Fig. 2.2 shows the capacity analysis for a non-i.i.d. DF cooperative network for varying decoding thresholds, γ_T. A local maximum is observed when ρ is near the γ_T value, and in the high SNR region, the effect of γ_T on the capacity is negligible. This local maximum in capacity is a result of the change in the average number of relays forwarding the source signal to the destination. The figure also shows the channel capacity achieved through the comparable AF cooperative net-

work. Clearly, the DF cooperative network performed better in terms of the channel capacity.

Fig. 2.4 shows the variation of the average number of relays forwarding the source signal, $\tilde{N}$, against ρ for different γ_T. For $\gamma_T = 15\,\text{dB}$, on average no relays forward signals to the destination ($\tilde{N} \leq 0.5$) until $\rho > 17\,\text{dB}$ and for $17\,\text{dB} < \rho < 35\,\text{dB}$, $\tilde{N}$ gradually increases from 0.5 to 2. This observation explains why the capacity curve for $\gamma_T = 15\,\text{dB}$ in Fig. 2.2 has a higher gradient for $0 < \rho < 17\,\text{dB}$ followed by a local maximum and a lower gradient for $17\,\text{dB} < \rho$. Similar results were obtained for the network with i.i.d. wireless channels.

2.6 Summary

Channel capacity through rate adaptive transmission for a cooperative network was investigated. The proposed system model and wireless channel model for the DF and AF cooperative networks were discussed in detail. The PDF of the total received SNR was derived. Analytical expressions for the channel capacity under optimal rate adaption with constant power were derived. The theoretical channel capacity derivations were compared with the results obtained from the Monte Carlo semi-analytical simulation. The channel capacity under DF cooperation (with the assumption of error-free decoding) was found to be better than the AF cooperation.
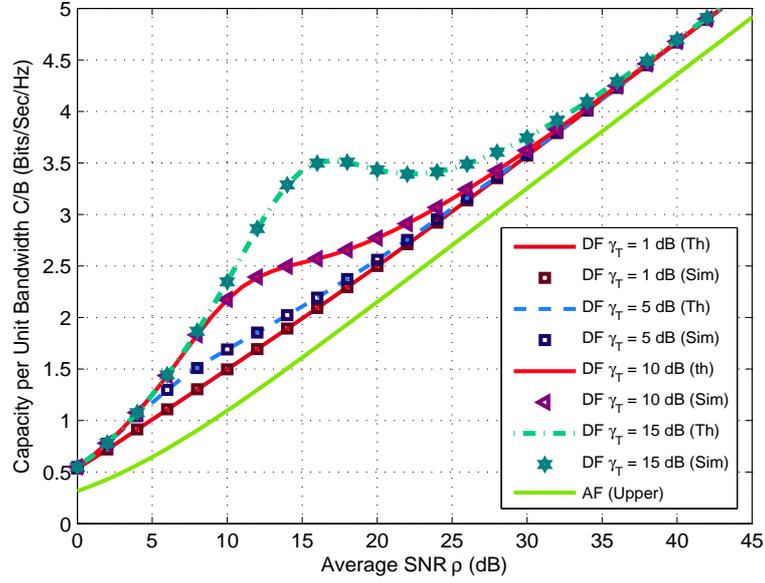
Figure 2.2: Capacity comparison of ORA scheme for DF relay networks with varying thresholds and non-i.i.d. fading.
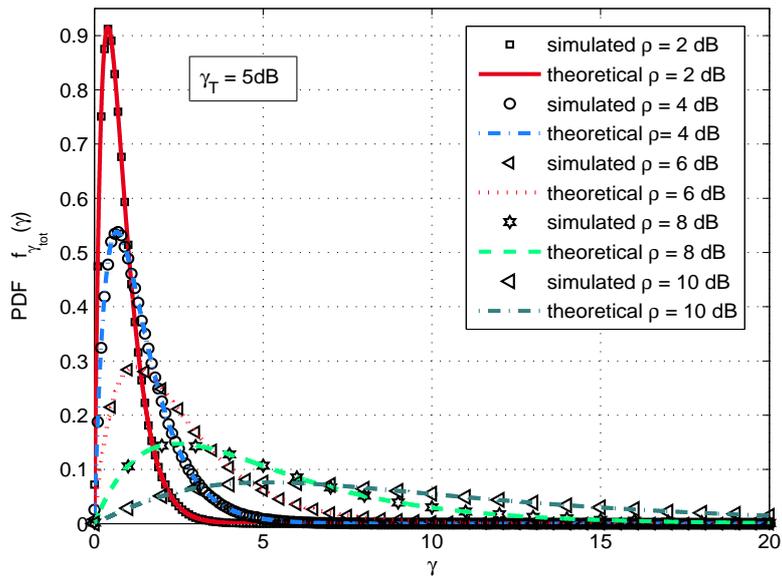
Figure 2.3: PDF of the total received SNR $f_{\gamma_{\text{tot}}}(\gamma)$ at destination for different average SNR values ($\gamma_T = 5$ dB).
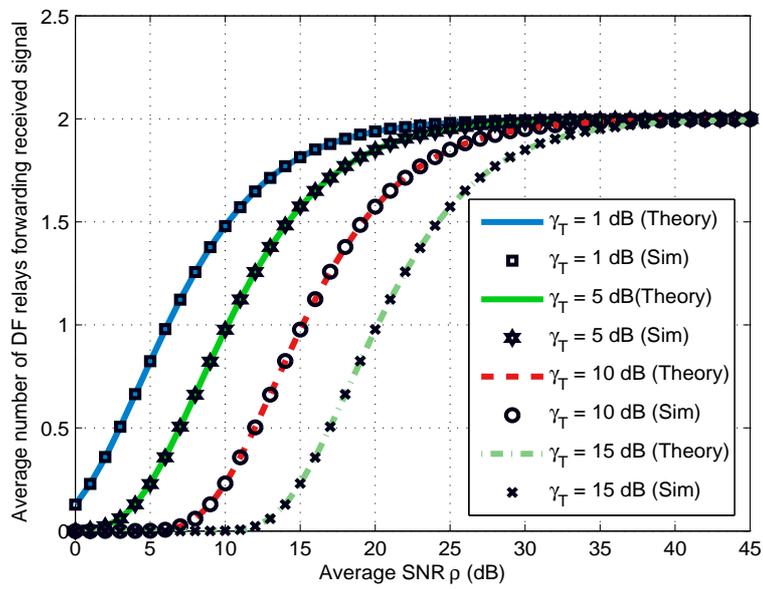
Figure 2.4: Average number of DF relays forwarding received signal to destination for different γ_T.

Chapter 3

Constant Power Rate Adaptation using Adaptive M-QAM

3.1 Introduction

In Chapter 2, the channel capacity for AF and DF cooperative networks was theoretically analyzed. Closed-form expressions were derived for the capacity under both i.i.d. and non-i.i.d. fading conditions. In this chapter, the performance of a practical rate adaptive transmission scheme with a cooperative network is analyzed[1]. An adaptive M-ary quadrature modulation (AMQAM) scheme consisting of a discrete set of transmission modes is considered for this purpose. The DF cooperative network (Chapter 2) and this rate adaptive scheme are analyzed for i.i.d. and non-i.i.d. fading conditions. The performance of the system under fixed and optimized SNR switching thresholds is investigated. The optimized switching thresholds required for AMQAM are computed for i.i.d. and non-i.i.d. Nakagami-m conditions by using the Lagrangian optimization approach [52].

The remainder of the chapter is organized as follows. Section 3.2 details the system and channel model. Section 3.3 describes the adaptive scheme employed, and Section 3.4 defines the performance parameters and includes their theoretical derivations for i.i.d. and non-i.i.d. fading environments. Section 3.5 explains how the switching thresholds for AMQAM are derived, and, finally, section 3.6 provides

---

[1]A version of this chapter has been accepted for publication in the proceedings of the IEEE International Conference on Communications (ICC) 2009 held in Dresden, Germany [38].

the numerical results obtained by using Monte Carlo simulations and the derived theoretical expressions.

3.2   Channel and System Model

Nakagami-m fading is assumed for all channels. The performance is analyzed for a DF cooperative network under both i.i.d. and non-i.i.d. fading conditions. The DF cooperative network (Fig. 2.1) is described in Section 2.3.2.

3.3   Rate Adaptive M-QAM

Rate adaptive transmission is implemented by using a discrete set of transmission modes. Each mode consists of a modulation scheme capable of supporting a different data rate. The transmission mode is changed based on CSI estimation at the destination. The CSI are fed back to the source transmitter via a reliable, low-latency feedback channel. Under this adaptive scheme, the source transmits at a constant average power and varies the data rate depending on the CSI.

In the subsequent analysis, the transmission mode is selected based on the received SNR at the destination. The range of the received SNR is partitioned into K regions by using a set of switching levels $\mathbf{S} = \{\gamma_n | n = 0, 1, ..., K\}$ with $K = 5$ being considered for our analysis. This system is termed **five-mode** AMQAM [52]. The transmitter selects mode n when the received SNR falls in the n-th region; i.e. $\gamma_n \leq \gamma_{tot} < \gamma_{n+1}$. The index of the selected transmission mode, n, is sent to the source through a reliable and low-delay feedback link (Fig. 2.1). The destination-to-source feedback link is assumed to be error-free. When the transmitter switches between different modes, the relays need to identify the correct mode. The transmitter may have to send side information to the relays, or, potentially, the relays may employ automatic modulation classification techniques [53, 54] to identify the incoming modulation mode without side information. Error-free decoding is assumed at the DF relays. The effect of decoding errors at the relays is investigated in Chapter 4. The PDFs derived for the i.i.d. and non-i.i.d. channel conditions

(Section 2.3.2) are used for our analysis.

Table 3.1 gives the parameters of the five-mode AMQAM scheme, where b_n is the number of bits per a transmitted symbol, γ is the instantaneous received SNR, and M_n is the constellation size of the modulation scheme used. The modulation schemes BPSK, QPSK, 16-QAM, and 64-QAM have been considered in four of the five modes since they have been widely used in many existing standards [9,55]. They have also been extensively studied in the literature under adaptive modulation [15, 36, 52, 56, 57].

3.4   System Performance Parameters

This section presents the parameters used to analyze the performance of the system. Since the operation of the adaptive scheme involves the selection of modes according to the prevailing channel conditions, a transmission mode selection probability (MSP) is defined as [52]

$$
\begin{aligned}
\delta_n &= \Pr(\gamma_n \leq \gamma < \gamma_{n+1}) \\
&= \int_{\gamma_n}^{\gamma_{n+1}} f_{\gamma_{tot}}(\gamma)\, d\gamma \,.
\end{aligned}
\tag{3.1}
$$

The quantity δ_n is the probability that the received SNR falls in the n-th region. By substituting the PDF of γ_{tot} for the i.i.d. fading environment given in (2.13) into (3.1), the MSP can be derived as

$$
\delta_n = \sum_{i=0}^{N} \binom{N}{i} \left[\frac{\Gamma(m, \frac{m\gamma_T}{\bar{\gamma}})}{\Gamma(m)} \right]^i \left[\frac{\gamma(m, \frac{m\gamma_T}{\bar{\gamma}})}{\Gamma(m)} \right]^{N-i} \left[\frac{\Gamma(m(i+1), \frac{m\gamma_n}{\bar{\gamma}}) - \Gamma(m(i+1), \frac{m\gamma_{n+1}}{\bar{\gamma}})}{\Gamma(m(i+1))} \right].
\tag{3.2}
$$

Similarly, the MSP for non-i.i.d. Nakagami-m fading can be derived by substituting (2.24) into (3.1) as

$$
\begin{aligned}
\delta_n = \sum_{k=0}^{2^N-1} \Pr(\mathbf{b}_k) \Bigg[&\sum_{j=1}^{m_{s,d}} \frac{\Delta_j(\mathbf{b}_k)}{(j-1)!} \left[\Gamma\left(j, \frac{m_{s,d}\,\gamma_n}{\bar{\gamma}_{s,d}}\right) - \Gamma\left(j, \frac{m_{s,d}\,\gamma_{n+1}}{\bar{\gamma}_{s,d}}\right) \right] \\
&+ \sum_{i=1,b_i \neq 0}^{N} \sum_{j=1}^{m_{i,d}} \frac{\Psi_{ij}(\mathbf{b}_k)}{(j-1)!} \left[\Gamma\left(j, \frac{m_{i,d}\,\gamma_n}{\bar{\gamma}_{i,d}}\right) - \Gamma\left(j, \frac{m_{i,d}\,\gamma_{n+1}}{\bar{\gamma}_{i,d}}\right) \right] \Bigg].
\end{aligned}
\tag{3.3}
$$

3.4.1 Outage Probability

According to the parameters given in Table 3.1, no transmission takes place when the received SNR falls in region 0. The probability of such an outage of transmission is given by

$$P_{out} = \Pr(\gamma_0 \le \gamma < \gamma_1) = \delta_0 \,. \tag{3.4}$$

By using (3.2) and (3.4), the outage probability for the i.i.d. case can be found as

$$P_{out} = 1 - \sum_{i=0}^{N} \binom{N}{i} \left[\frac{\Gamma(m, \frac{m\gamma_T}{\bar{\gamma}})}{\Gamma(m)} \right]^i \left[\frac{\gamma(m, \frac{m\gamma_T}{\bar{\gamma}})}{\Gamma(m)} \right]^{N-i} \left[\frac{\Gamma(m(i+1), \frac{m\gamma_1}{\bar{\gamma}})}{\Gamma(m(i+1))} \right]. \tag{3.5}$$

Similarly, by using (3.3) and (3.4), the outage probability for the non-i.i.d. case is found as

$$
\begin{aligned}
P_{out} &= 1 - \sum_{k=0}^{2^N-1} \Pr(\mathbf{b}_k) \left[\sum_{j=1}^{m_{s,d}} \frac{\Delta_j(\mathbf{b}_k)}{(j-1)!} \left[\Gamma\left(j, \frac{m_{s,d}\,\gamma_1}{\bar{\gamma}_{s,d}}\right) \right] \right. \\
&\quad \left. + \sum_{i=1,b_i \ne 0}^{N} \sum_{j=1}^{m_{i,d}} \frac{\Psi_{ij}(\mathbf{b}_k)}{(j-1)!} \left[\Gamma\left(j, \frac{m_{i,d}\,\gamma_1}{\bar{\gamma}_{i,d}}\right) \right] \right].
\end{aligned}
\tag{3.6}$$

3.4.2 Average Spectral Efficiency

The average spectral efficiency achieved by the system can be expressed as the sum of the data rates b_n in each region weighted by the MSP of each region, which is [15, 52, 58]

$$\frac{R}{B} = \frac{1}{\tilde{N}+1} \sum_{n=1}^{K-1} b_n \delta_n \,, \tag{3.7}$$

where $b_n = \log_2(M_n)$ is the data rate of the nth region, B is the bandwidth, R is the average throughput, and $\tilde{N}$ is the average number of DF relay nodes forwarding the source signal to the destination. The division by $(\tilde{N}+1)$ accounts for the fact that transmission takes place by using $(\tilde{N}+1)$ orthogonal channels. By using (3.2) and (3.7), the average spectral efficiency for an i.i.d. fading environment can be

Table 3.1: Five-Mode Adaptive M-QAM Parameters

SNR	n	M_n	b_n	$mode$
$\gamma_0 \leq \gamma < \gamma_1$	0	0	0	No Tx
$\gamma_1 \leq \gamma < \gamma_2$	1	2	1	BPSK
$\gamma_2 \leq \gamma < \gamma_3$	2	4	2	QPSK
$\gamma_3 \leq \gamma < \gamma_4$	3	16	4	16-QAM
$\gamma_4 \leq \gamma < \gamma_5$	4	64	6	64-QAM

expressed as

$$
\frac{R}{B} = \sum_{n=1}^{K-1} b_n \sum_{i=0}^{N} \frac{\binom{N}{i}}{(i+1)} \left[\frac{\Gamma\left(m, \frac{m\gamma_T}{\bar{\gamma}}\right)}{\Gamma(m)} \right]^i \left[\frac{\gamma\left(m, \frac{m\gamma_T}{\bar{\gamma}}\right)}{\Gamma(m)} \right]^{N-i}
$$
$$
\times \left[\frac{\Gamma\left(m(i+1), \frac{m\gamma_n}{\bar{\gamma}}\right) - \Gamma\left(m(i+1), \frac{m\gamma_{n+1}}{\bar{\gamma}}\right)}{\Gamma(m(i+1))} \right]. \quad (3.8)
$$

Similarly, by using (3.3) and (3.7), the average spectral efficiency for non-i.i.d. fading can be expressed as

$$
\frac{R}{B} = \sum_{n=1}^{K-1} b_n \sum_{k=0}^{2^N-1} \Pr(\underline{\mathbf{b}}_k) \left[1 + \sum_{i=1}^{N} b_i \right]^{-1}
$$
$$
\times \left[\sum_{j=1}^{m_{s,d}} \frac{\Delta_j(\mathbf{b}_k)}{(j-1)!} \left[\Gamma\left(j, \frac{m_{s,d}\,\gamma_n}{\bar{\gamma}_{s,d}}\right) - \Gamma\left(j, \frac{m_{s,d}\,\gamma_{n+1}}{\bar{\gamma}_{s,d}}\right) \right] \right. \quad (3.9)
$$
$$
\left. + \sum_{i=1,b_i \neq 0}^{N} \sum_{j=1}^{m_{i,d}} \frac{\Psi_{ij}(\mathbf{b}_k)}{(j-1)!} \left[\Gamma\left(j, \frac{m_{i,d}\,\gamma_n}{\bar{\gamma}_{i,d}}\right) - \Gamma\left(j, \frac{m_{i,d}\,\gamma_{n+1}}{\bar{\gamma}_{i,d}}\right) \right] \right].
$$

3.4.3 Average BER

Since AMQAM is transmitted by using a discrete set of modes, the average BER reflects the bit errors of each individual mode of transmission. The total average bit error rate will depend both on the modulation scheme used in each mode and on the probability that each mode is used for transmission. Hence, the average BER for the five-mode AMQAM scheme is given as [15, 52]

$$BER_{avg} = \frac{\sum\limits_{n=1}^{K-1} b_n\, P_n}{\sum\limits_{n=1}^{K-1} b_n \delta_n}, \tag{3.10}$$

where P_n is the BER of the n-th transmission mode, which is calculated as

$$P_n = \int_{\gamma_n}^{\gamma_{n+1}} P_{M_n,QAM}(\gamma) f_{\gamma_{tot}}(\gamma)\, d\gamma. \tag{3.11}$$

$P_{M_n,QAM}$ is the BER of square M-QAM in an AWGN channel, with coherent detection and Gray coding given as [52]

$$P_{M_n,QAM} = \sum_l A_l\, Q(\sqrt{a_l \gamma}), \tag{3.12}$$

where $Q(\cdot)$ is the standard Gaussian Q-function defined as $Q(x) = \frac{1}{\sqrt{2\pi}} \int_x^\infty e^{-z^2/2}\, dz$, γ is the received SNR, and A_l and a_l are constants particular to the QAM constellation used [52].

By using (2.13), (3.11) and (3.12), the expression for P_n can be derived as

$$
\begin{aligned}
P_n &= \int_{\gamma_n}^{\gamma_{n+1}} \left[\sum_l A_l\, Q(\sqrt{a_l \gamma}) \right] \left[\sum_{i=0}^{N} \binom{N}{i} \left[\frac{\Gamma\left(m, \frac{m\gamma_T}{\bar{\gamma}}\right)}{\Gamma(m)} \right]^i \left[\frac{\gamma\left(m, \frac{m\gamma_T}{\bar{\gamma}}\right)}{\Gamma(m)} \right]^{N-i} \right. \\
&\quad \times \left. \left(\frac{m}{\bar{\gamma}} \right)^{m(i+1)} \frac{\gamma^{m(i+1)-1}}{(m(i+1)-1)!} e^{-\frac{m\gamma}{\bar{\gamma}}} \right] d\gamma \\
&= \sum_{i=0}^{N} \binom{N}{i} \left[\frac{\Gamma\left(m, \frac{m\gamma_T}{\bar{\gamma}}\right)}{\Gamma(m)} \right]^i \left[\frac{\gamma\left(m, \frac{m\gamma_T}{\bar{\gamma}}\right)}{\Gamma(m)} \right]^{N-i} \\
&\quad \times \frac{\left(\frac{m}{\bar{\gamma}} \right)^{m(i+1)}}{(m(i+1)-1)!} \sum_l A_l \int_{\gamma_n}^{\gamma_{n+1}} Q(\sqrt{a_l \gamma})\, \gamma^{m(i+1)-1}\, e^{-\frac{m\gamma}{\bar{\gamma}}}\, d\gamma.
\end{aligned} \tag{3.13}
$$

Let

$$I_i(a_l, \beta, \gamma_n, \gamma_{n+1}) = \int_{\gamma_n}^{\gamma_{n+1}} Q(\sqrt{a_l \gamma})\, \gamma^{m(i+1)-1}\, e^{-\beta\gamma}\, d\gamma. \tag{3.14}$$

From our previous work in [15], $I_i(a_l, \beta, \gamma_n, \gamma_{n+1})$ can be written in closed form as

$$
\begin{aligned}
I_i(a_l, \beta, \gamma_n, \gamma_{n+1}) \;=\; & Q(\sqrt{a_l\gamma})\beta^{-i}(i-1)! \left[1 - e^{-\beta\gamma}\sum_{r=0}^{i-1}\frac{(\beta\gamma)^r}{r!}\right]\Bigg|_{\gamma_n}^{\gamma_{n+1}} \\
& -\frac{1}{2}\beta^{-i}(i-1)!\Bigg\{ (\pi)^{-0.5}\Gamma(0.5, \frac{\gamma a_l}{2})\Big|_{\gamma_n}^{\gamma_{n+1}} \\
& -\sqrt{\frac{a_l}{2\pi}}\sum_{r=0}^{i-1}\frac{\beta^r}{r!}(a_l/2+\beta)^{-r-0.5} \\
& \times \Gamma(r+0.5, (a_l/2+\beta)\gamma)\Big|_{\gamma_n}^{\gamma_{n+1}} \Bigg\}.
\end{aligned}
\tag{3.15}
$$

Hence, by substituting (3.15) into (3.13), the closed form expression for P_n can be written as

$$
\begin{aligned}
P_n \;=\; & \sum_{i=0}^{N}\binom{N}{i}\left[\frac{\Gamma\left(m, \frac{m\gamma_T}{\bar{\gamma}}\right)}{\Gamma(m)}\right]^i \left[\frac{\gamma\left(m, \frac{m\gamma_T}{\bar{\gamma}}\right)}{\Gamma(m)}\right]^{N-i} \\
& \times \frac{\left(\frac{m}{\bar{\gamma}}\right)^{m(i+1)}}{(m(i+1)-1)!}\sum_l A_l\, I_{m(i+1)}(a_l, m/\bar{\gamma}, \gamma_n, \gamma_{n+1}).
\end{aligned}
\tag{3.16}
$$

Similarly, by using equations (2.24), (3.11) and (3.15), the closed form expression for P_n for the non-i.i.d. case can be derived as

$$
\begin{aligned}
P_n \;=\; & \sum_{k=0}^{2^N-1}\Pr(\underline{\mathbf{b}}_k)\Bigg[\sum_{j=1}^{m_{s,d}}\frac{\Delta_j(\mathbf{b}_k)}{(j-1)!}\left(\frac{m_{s,d}}{\bar{\gamma}_{s,d}}\right)^j\sum_l A_l\, I_j(a_l, m_{s,d}/\bar{\gamma}_{s,d}, \gamma_n, \gamma_{n+1}) \\
& + \sum_{i=1, b_i\neq 0}^{N}\sum_{j=1}^{m_{i,d}}\frac{\Psi_{ij}(\mathbf{b}_k)}{(j-1)!}\left(\frac{m_{i,d}}{\bar{\gamma}_{i,d}}\right)^j\sum_l A_l\, I_j(a_l, m_{i,d}/\bar{\gamma}_{i,d}, \gamma_n, \gamma_{n+1})\Bigg].
\end{aligned}
\tag{3.17}
$$

By substituting for P_n and δ_n in (3.10) by using (3.2), (3.16) and (3.3), (3.17), the average BER can be obtained for the i.i.d Nakagami and non-i.i.d. Nakagami fading cases, respectively.

3.5 Switching Levels for Mode Selection

The operation of the five-mode AMQAM described in Section 3.3 relies heavily on the switching levels used to partition the received SNR into the five regions, one

for each transmission mode. The switching levels are determined so that a QoS constraint is maintained while rate adaptation is performed. We have considered the adaptation policy introduced in [52] where a target BER level is used as the QoS constraint.

We next discuss two types of switching level assignment for the five-mode AMQAM scheme used in the cooperative network: (1) fixed switching levels and (2) optimized switching levels. In both methods, rate adaptation is performed to increase the throughput while satisfying the required target BER level.

3.5.1 Fixed Switching Levels

In this method, a fixed set of switching levels is used to partition the received SNR. Each switching level is chosen so that the two modes being separated by the switching level satisfy the BER constraint under AWGN conditions at the SNR value of switching. Particularly, the higher of the two modes should yield a BER approximately equal to the BER target. We have adopted the criteria used in [58] for determining the fixed switching levels:

$$
\begin{aligned}
\gamma_0 &= 0 \\
\gamma_1 &= [\mathrm{erfc}^{-1}(2\mathrm{BER}_0)]^2, \\
\gamma_n &= \tfrac{2}{3}K_0(M_n - 1); \quad n = 2, 3, \ldots, K-1, \\
\gamma_K &= +\infty,
\end{aligned}
\tag{3.18}
$$

where BER_0 is the target BER level, $\mathrm{efrc}^{-1}(\cdot)$ is the inverse complementary error function, and $K_0 = -\ln(5\,\mathrm{BER}_0)$.

3.5.2 Optimized Switching Levels

The fixed switching level assignment discussed earlier provides an easy method for allocating SNR regions for each transmit mode to operate on. The average BER obtained through this technique is very conservative with respect to the target level, which is discussed in Section 3.6. However, by making further adjustments to the switching levels, the spectral efficiency can be increased while maintaining the BER target.
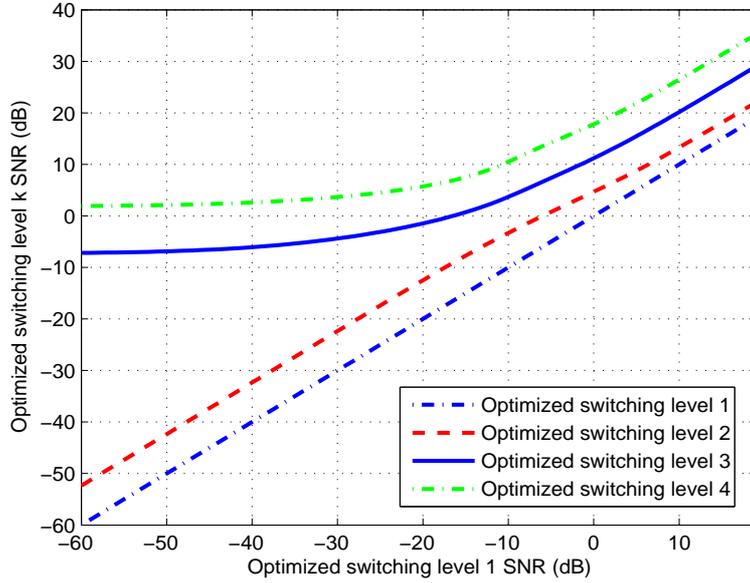
Figure 3.1: Relationship between optimized switching levels

In [52], Choi and Hanzo showed that the switching levels could be optimally adjusted for a given average SNR so that the total average BER was exactly equal to the target BER level. The optimization was performed so that the average throughput, $\sum_{n=1}^{K-1} b_n \, \delta_n$, was maximized under the constraint of $BER_{avg} = \text{BER}_0$, where BER_0 was the target BER level. Here, both the average throughput and the average bit error rate BER_{avg} are functions of the average SNR. Since any set of switching levels $s \in \mathbf{S}$ consists of $K-1$ independent variables ($\gamma_0 = 0$ and $\gamma_K = \infty$ are fixed), the optimization process amounts to a $K-1$ dimensional optimization problem under the BER constraint. The results of [52] show that any set of optimized switching levels $\hat{s} \in \mathbf{S}$ is a function of the first optimized switching level $\hat{\gamma}_1$ and is independent of the underlying propagation environment. These results reduce the multi-dimensional optimization problem to a one-dimensional optimization. For the five-mode operation, $(K = 5)$, the relationship between $\hat{\gamma}_1$ and the rest of the optimized switching levels, $\hat{\gamma}_2, \hat{\gamma}_3$ and $\hat{\gamma}_4$, is given in [52, Fig. 4] and is reproduced in Fig. 3.1 for clarity. The set of optimized switching levels for a particular average SNR $\bar{\gamma}$ and target BER level BER_0 is found by solving the constraint function given

by [52]

$$Y(\bar{\gamma}; \hat{\boldsymbol{s}}(\hat{\gamma}_1)) = \sum_{n=1}^{N} b_n P_n - \mathrm{BER}_0 \sum_{n=1}^{N} b_n \delta_n = 0 \,, \qquad (3.19)$$

where $\hat{\boldsymbol{s}}(\hat{\gamma}_1)$ is the set of optimum switching levels as a function of $\hat{\gamma}_1$. A set of optimized switching levels exists only when there is a solution to $Y(\bar{\gamma}; \hat{\boldsymbol{s}}(\hat{\gamma}_1)) = 0$. By using the relationship between the switching levels given in Fig. 3.1 and the MSP (3.2), (3.3) and the mode-specific BER (3.16), (3.17) and solving for $Y(\bar{\gamma}; \hat{\boldsymbol{s}}(\hat{\gamma}_1)) = 0$ numerically, a unique set of optimized switching levels $\hat{\boldsymbol{s}}$ is found for a given $\bar{\gamma}$. The optimized switching levels derived are presented in Fig. 3.2 and Fig. 3.3 for the i.i.d. and non-i.i.d. channel conditions together with the corresponding fixed switching levels.

3.6 Numerical Results

This section presents a comparison of the analytical and simulation results for the performance parameters of Section 3.4. The results for outage probability, mode selection probability, average BER, and achievable spectral efficiency are presented for fixed and optimum switching level assignments. For the i.i.d. Nakagami-m fading case, a two-relay cooperative network is considered with fading parameter $m = 2$. In the non-i.i.d. case, a two-relay cooperative network with the following average SNR values and Nakagami fading parameters is considered: $\bar{\gamma}_{s,d} = 0.5\rho$, $\bar{\gamma}_{s,1} = 0.2\rho$, $\bar{\gamma}_{s,2} = 0.7\rho$, $\bar{\gamma}_{1,d} = 0.9\rho$, $\bar{\gamma}_{2,d} = 0.4\rho$, $m_{s,d} = 2$, $m_{s,1} = 1$, $m_{s,2} = 2$, $m_{1,d} = 3$, $m_{2,d} = 1$ where ρ is average SNR. The decoding threshold γ_T for the DF cooperative network is set to be 5 dB, and the target BER for rate adaptation is considered to be $\mathrm{BER}_0 = 1 \times 10^{-3}$.

Fig. 3.2 and Fig. 3.3 show the optimized and fixed switching levels for the i.i.d and non-i.i.d. cases. For a small average SNR, the difference between the fixed and the optimized switching levels is fairly small, but the difference progressively increases as the average SNR increases. At a particular SNR value known as the **avalanche** SNR [52], all the optimum switching levels abruptly reach zero. This event occurs when the BER of the highest order modulation scheme equals the
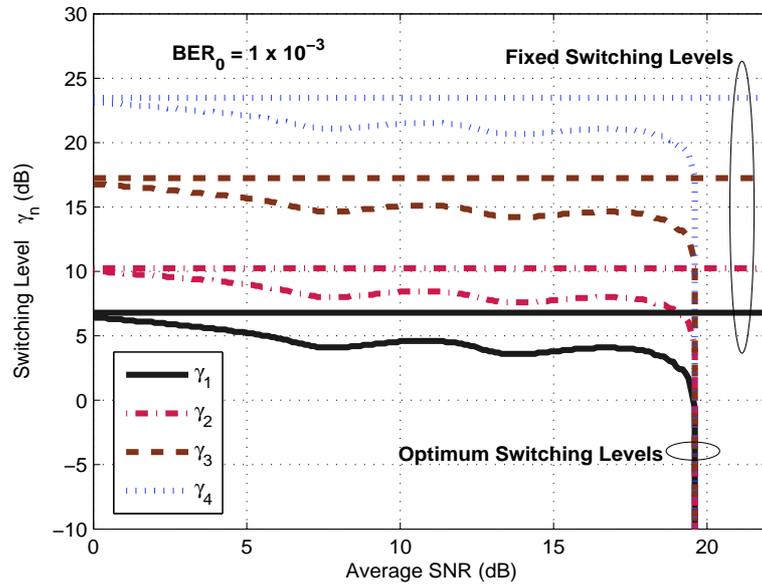
Figure 3.2: Switching levels for i.i.d. Nakagami-m fading ($m = 2$), for a two relay network.
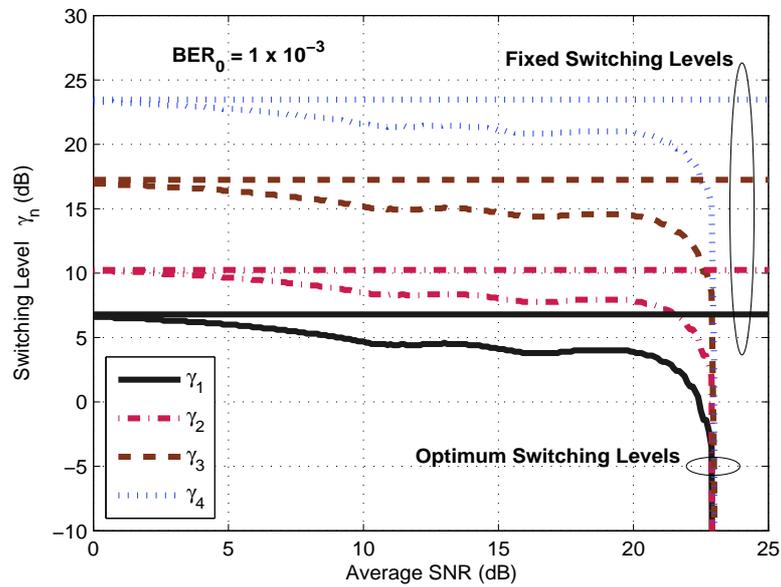
Figure 3.3: Switching levels for non-i.i.d. Nakagami-m fading and for a two relay network.

target BER, after which adaptation is abandoned, and modulation is performed by using the highest order modulation scheme. The avalanche SNR for the i.i.d. case

is around 19 dB, and for the non-i.i.d. case is 23 dB.

Figure 3.4: Probability of mode selection with fixed switching levels for i.i.d. Nakagami-m fading ($m = 2$), for a two relay network.

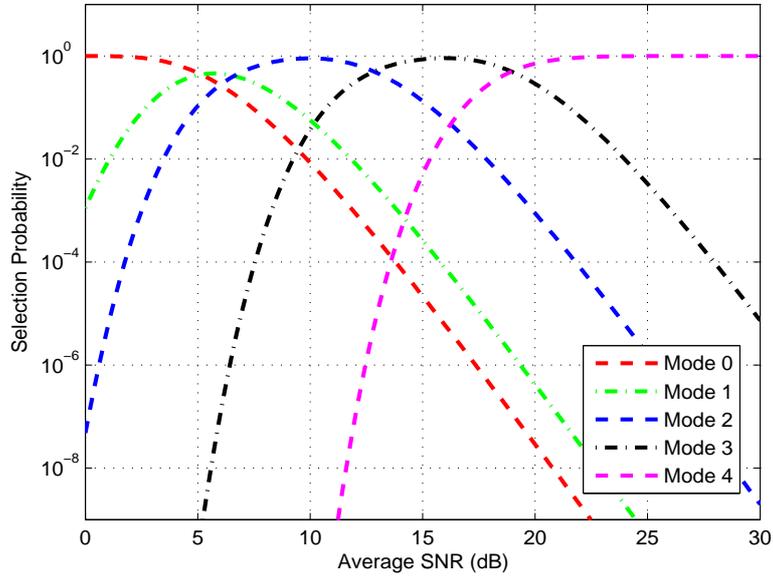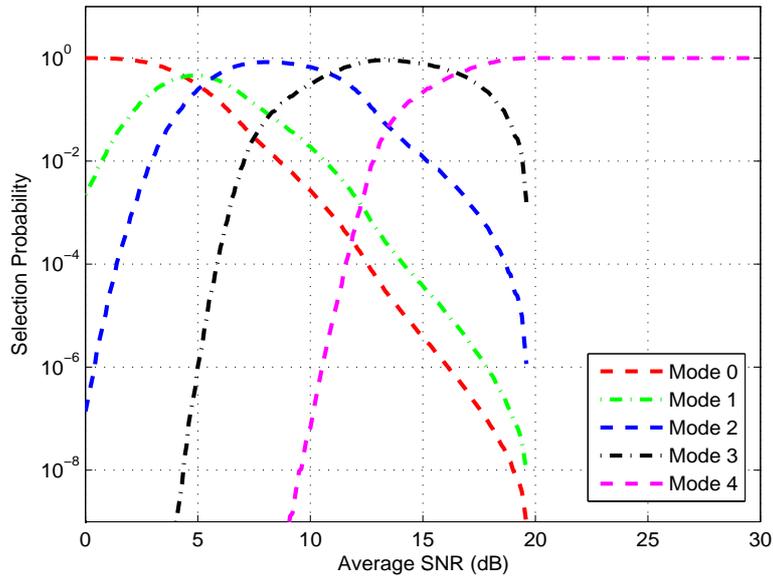Figure 3.5: Probability of mode selection with optimized switching levels for i.i.d. Nakagami-m fading ($m = 2$), for a two relay network.

The probability of the transmitter selecting different transmission modes is shown

in Fig. 3.4 and 3.5 for the fixed switching levels and the optimized switching levels for i.i.d. channel conditions. Fig. 3.4 reveals that for fixed switching at a low average SNR, transmission occurs mainly using mode 1 (BPSK) whereas at a high average SNR, the transmitter resorts exclusively to mode 4 (64 - QAM) with the highest bit rate. Under this method, for any given average SNR there exists a certain probability of selection, however small it may be, for each mode of transmission. On the other hand, with optimized switching levels, when the average SNR values are less than the avalanche SNR, the variation of the mode selection probabilities with the average SNR is similar to that of the fixed switching method. However, when the average SNR equals the avalanche SNR, all modes, except for the highest one, cease to operate, resulting in their probability of selection to abruptly reach zero. With an average SNR beyond the avalanche SNR, only the highest mode operates. Similar observations were made under non-i.i.d. channel conditions.
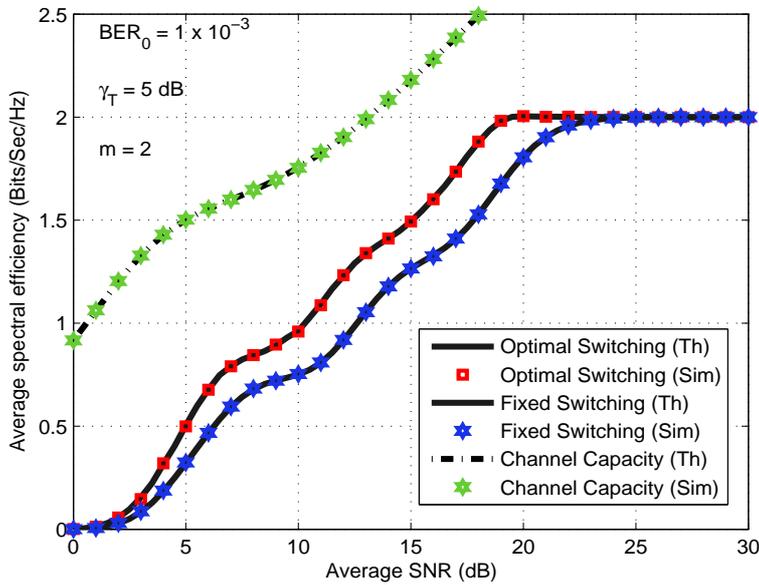
Figure 3.6: Average throughput for i.i.d. Nakagami-m fading ($m = 2$), for a two relay network.

The average spectral efficiency is plotted in Fig. 3.6 for the i.i.d. fading case. Optimum switching levels yield higher throughput for an equal average SNR. A performance gain of 2 - 3 dB is achieved when optimum switching levels are used
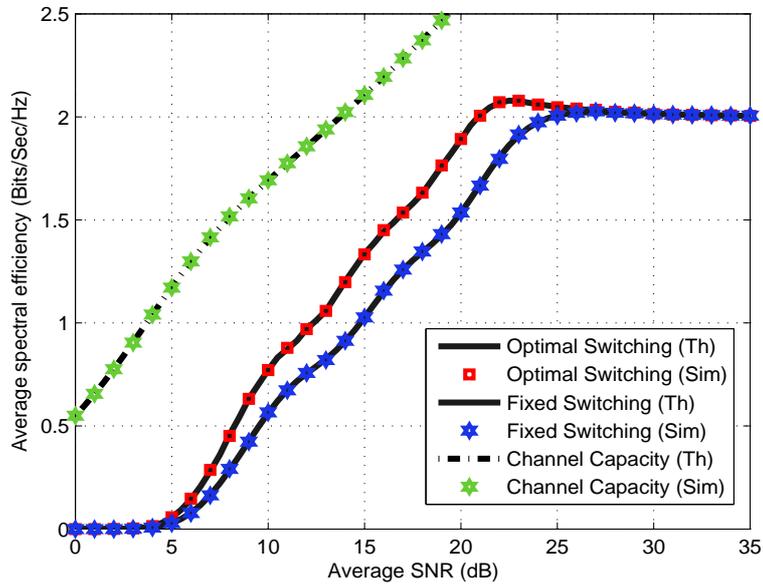
Figure 3.7: Average throughput for a two relay network with non-i.i.d. Nakagami-m fading.

as opposed to fixed switching levels. Similar observations can be made under the non-i.i.d. fading conditions, which are shown in Fig. 3.7.
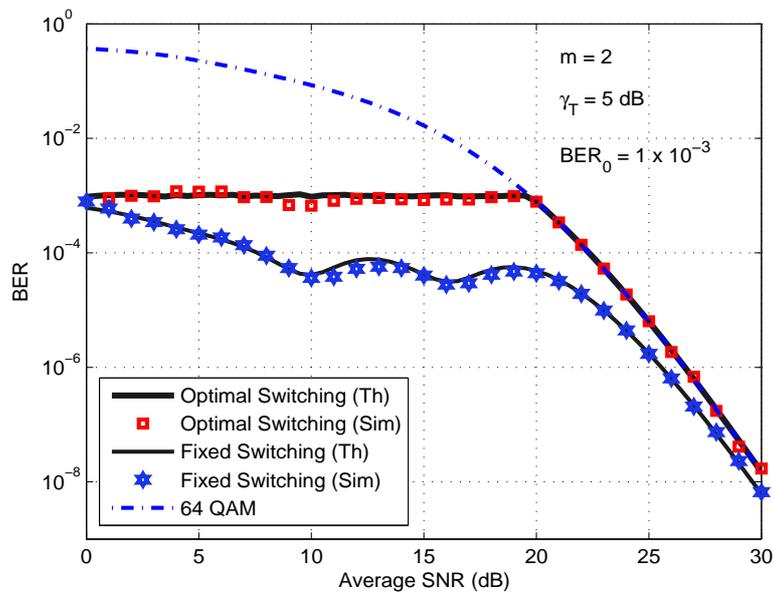
Figure 3.8: Average bit error rate for i.i.d. Nakagami-m fading ($m = 2$), for a two relay network.
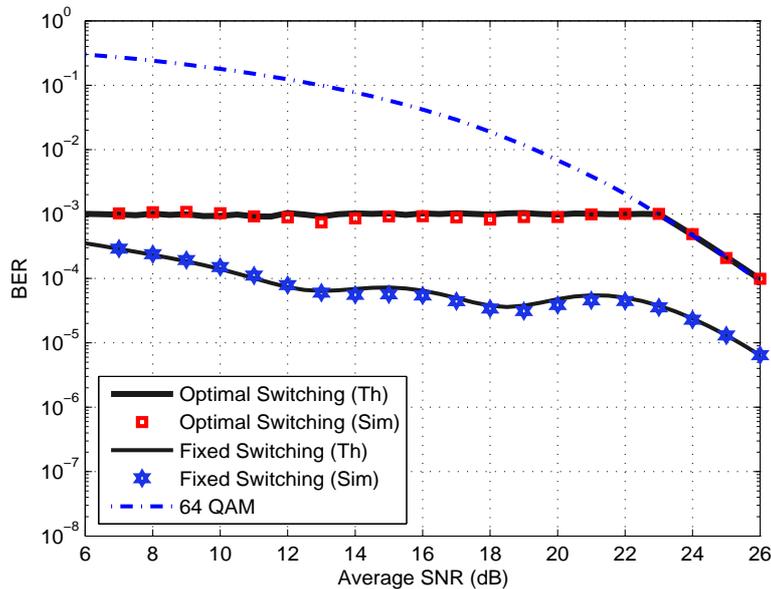
Figure 3.9: Average bit error rate for a two relay network with non-i.i.d. Nakagami-m fading.

Fig. 3.8 provides the average BER performance analysis in i.i.d. fading conditions. The system using the optimized switching levels maintains the target BER requirement until the avalanche SNR is reached, when the adaptive modulation is stopped, and the highest modulation scheme is used for transmission. Under fixed switching levels, the average BER of the five-mode AMQAM is always well below the target BER and hence satisfies the QoS requirement; however, this QoS conformance comes at the cost of sacrificing system performance in the form of the average throughput — see the plots of the average spectral efficiency in Fig. 3.2. Similar results are obtained under non-i.i.d. fading conditions (Fig. 3.9).

The outage probability is depicted in Fig. 3.10 and Fig. 3.11 for the i.i.d and non-i.i.d. cases. The system using optimized switching levels experiences less outage as compared to the system under fixed switching levels.
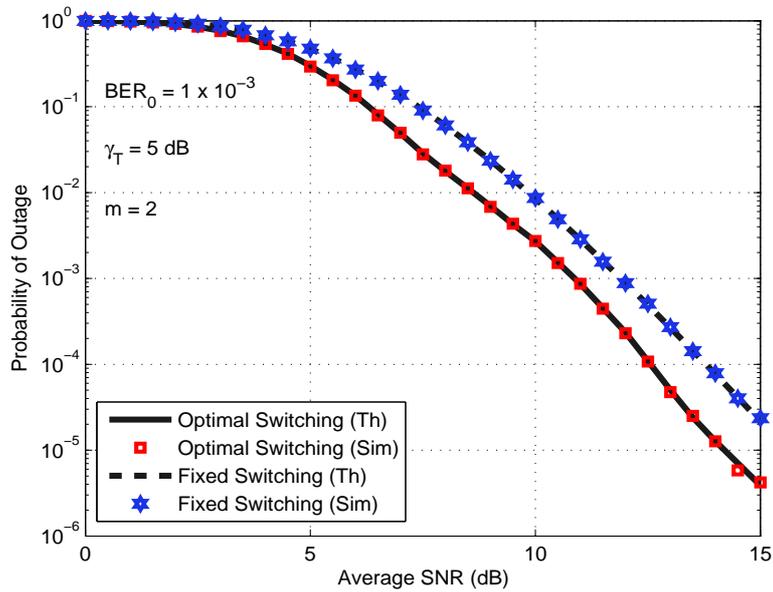
Figure 3.10: Outage probability for i.i.d. Nakagami-m fading ($m = 2$), for a two relay network.
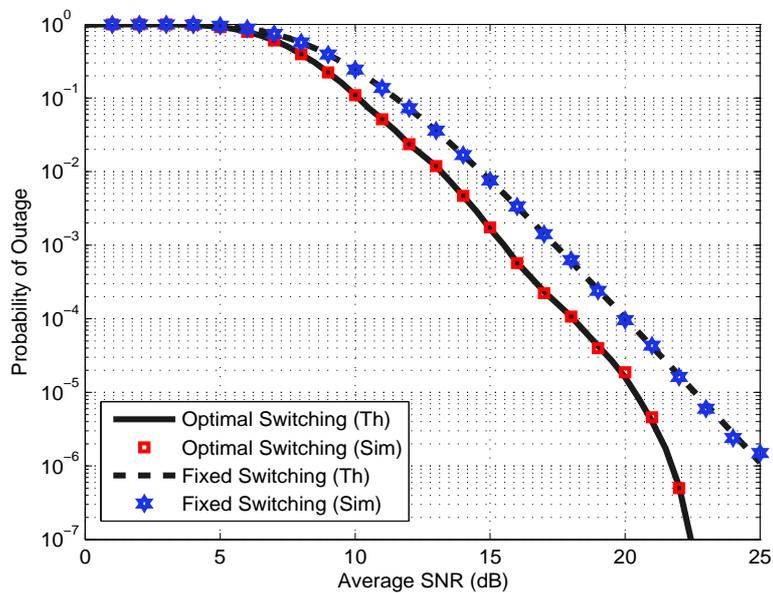
Figure 3.11: Outage probability for a two relay network with non-i.i.d. Nakagami-m fading.

3.7 Summary

A five-mode AMQAM was considered with a cooperative DF network. The performance metrics required to analyze this rate adaptive system on a cooperative DF

relay network were derived mathematically. The total system was tested for two methods of switching level assignment. The results obtained through simulation and numerically provided a good match and showed that the optimized switching level yielded the best system performance. On the other hand, the fixed switching level assignment provided a more conservative performance in terms of guaranteeing the required QoS.

Chapter 4

Rate Adaptation under Cooperative Demodulation

4.1   Introduction

The analysis of AMQAM in Chapter 3 was performed for error-free decoding at the relays. MRC at the destination then provides full diversity benefits. However, when the decoding errors at the relays are considered, MRC is no longer the optimal combining technique [59]. The error propagation via relays then leads to a degradation of performance. Hence, different techniques need to be considered for the combining of the signals received at the destination. In this chapter, we investigate the effect of the decoding errors at the relays on the performance of the system[1].

Chapter 4 is organized as follows. Section 4.2 presents a discussion of cooperative diversity combining techniques. The operation of C-MRC is discussed in detail, and the fitness of a proposed heuristic approximation for the total received SNR is validated by using simulation results. In Section 4.3, a cooperative network using C-MRC together with AMQAM is analyzed. Mathematical expressions are derived for performance metrics (mode selection probability, outage probability, average spectral efficiency and average BER) by using the PDF of the SNR approximation. The analytical expressions and simulation results are compared.

---

[1]A version of this chapter has been submitted for publication as a regular paper in the IEEE Transactions on Wireless Communications [39].

4.2 Cooperative Demodulation in DF Cooperative Networks

As mentioned before, in DF cooperative networks, the relays demodulate, decode, and retransmit the source signal. Decoding errors at the relays can cause error propagation. The use of MRC to combine the relayed signals at the destination is not optimal in this case. Techniques to optimally demodulate and detect the received signal by considering error propagation via relays are found in the literature. Reference [60] presents a maximal likelihood (ML) optimal detector for BPSK. The authors of [60] also provide a suboptimal combiner termed λ-MRC due to the complexity of the optimal detector. A piece-wise linear (PL) near-ML decoder is derived for coherent and non-coherent BFSK in [61]. Reference [62] provides a low-complexity method termed cooperative MRC (C-MRC), which tightly lower-bounds the performance of ML detection. Reference [63] presents the product MRC (P-MRC) scheme, which requires a significantly lower signaling overhead than that of C-MRC. Most of these techniques require the destination to have knowledge of the instantaneous CSI or BER at the relays.

4.2.1 Cooperative MRC

We have chosen the C-MRC scheme proposed in [62, 64] for the cooperative demodulation of the received signals at the destination because of this scheme's low complexity and near-ML performance. Furthermore, the implementation of ML detection for higher-order constellations, considered in our adaptive scheme, becomes exceedingly complicated with the presence of errors at the relays.

The combining of received signals $r_{s,d}$ and $r_{i,d}$, $i \in \{1, ..., N\}$ by using C-MRC is done as follows [62]:

$$r = w_{s,d}\, r_{s,d} + \sum_{i=1}^{N} w_{i,d}\, r_{i,d} \;, \tag{4.1}$$

where $w_{s,d}$ and $w_{i,d}$ are weights which are functions of $h_{s,d}$, $h_{s,i}$ and $h_{i,d}$. The weight $w_{s,d}$ is chosen to be $w_{s,d} = h_{s,d}^*$ as in the case of MRC. However, for determining

the weight $w_{i,d}$, which has to account for the errors introduced at the relay, the end-to-end equivalent SNR for the path via the ith relay is required. Hence, $w_{i,d}$ is chosen as

$$w_{i,d} = \frac{\gamma_{eq}}{\gamma_{i,d}} \, h_{i,d}^* \, , \qquad (4.2)$$

where γ_{eq} is the equivalent one-hop received SNR for the two-hop path via the ith relay. It was shown in [62,64] that γ_{eq} is bounded as $\gamma_{min} - \frac{3.24}{\alpha} < \gamma_{eq} \leq \gamma_{min}$ where $\gamma_{min} = \min(\gamma_{s,i}, \gamma_{i,d})$ and α is a constant dependent on the modulation scheme. Therefore, we have approximated γ_{eq} as

$$\gamma_{eq} \approx \min(\gamma_{s,i}, \gamma_{i,d}) \, .$$

Under this approximation, when $\gamma_{s,i} > \gamma_{i,d}$, $w_{i,d}$ reverts to conventional MRC, so that $w_{i,d} = h_{i,d}^*$; i.e., the combiner is more confident that the symbols arriving from the relay are accurate since the source-to-relay link is of higher quality than the relay-to-destination link. When $\gamma_{s,i} < \gamma_{i,d}$, the combiner has low confidence in the reliability of the symbol arriving at the relay.

The detected symbol at the destination $\hat{x}$ is given as

$$\hat{x} = \arg \min_{x \in A_x} \left| w_{s,d} \, r_{s,d} + \sum_{i=1}^{N} w_{i,d} \, r_{i,d} - \left(w_{s,d} \, h_{s,d} + \sum_{i=1}^{N} w_{i,d} \, h_{i,d} \right) x \right|^2 \, , \quad (4.3)$$

where A_x is the set of constellation points or symbols of the constellation considered for transmission. The analysis carried out in [62, 64] proves that C-MRC provides full diversity benefits at the destination. However, to use this cooperative demodulation scheme with the proposed AMQAM transmission under an average BER constraint, a relationship is required which links the CSI estimated ($\gamma_{s,i}, \gamma_{i,d}$ and $\gamma_{s,d}$), with the total instantaneous received SNR at the destination.

4.2.2   Approximation for Total received SNR

To use C-MRC in the AMQAM scheme described in Chapter 3, the instantaneous total received SNR at the destination is needed for selecting the appropriate modulation scheme. Under cooperative demodulation schemes such as C-MRC, which
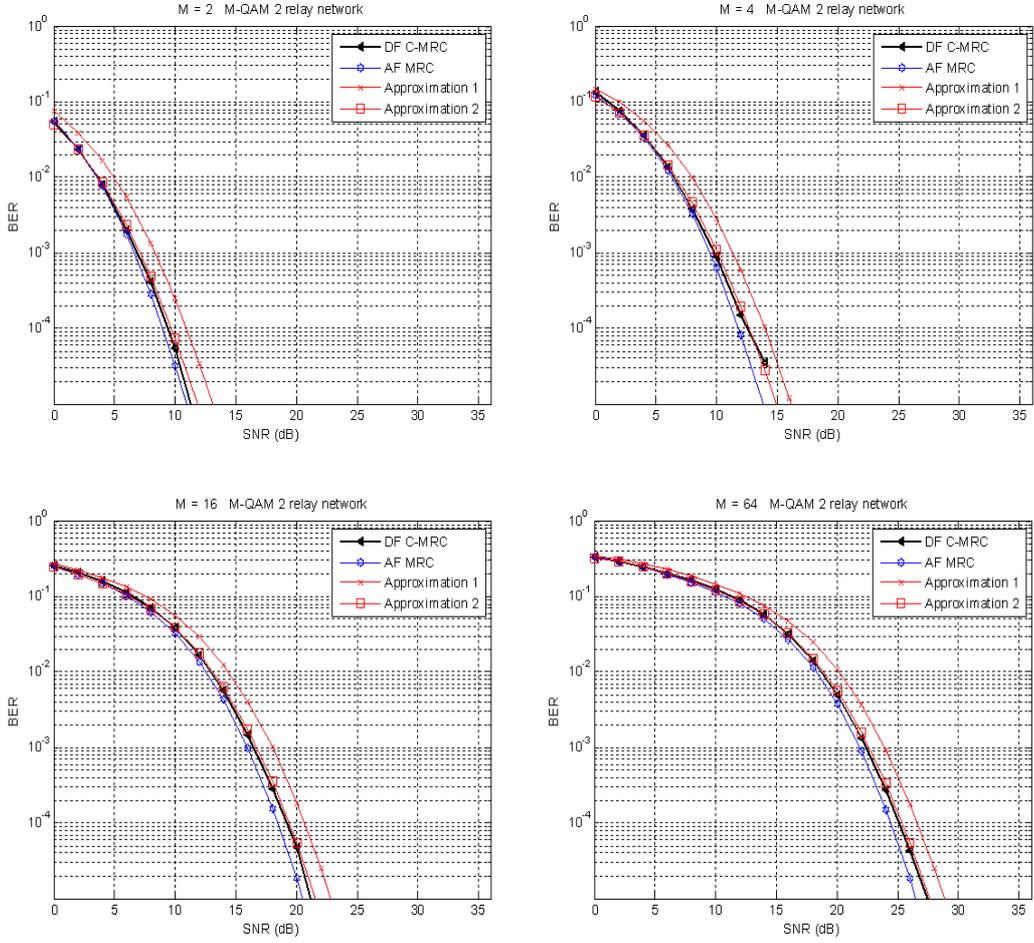
Figure 4.1: BER of 2 relay network under different M-QAM constellations with Nakagami-m fading, $m = 2$.

consider the effects of the decoding errors at the relays, the derivation of an analytical closed form expression for the total received SNR appears complicated or intractable. Also, such an expression may essentially be dependent on the modulation scheme used (since the bit errors caused at the relays depend on the modulation scheme employed). Hence, the use of C-MRC would complicate our application, which requires the received SNR to be independent of the modulation scheme, because the SNR is used to determine the transmission and reception mode.

Due to these difficulties in deriving an exact expression for the total received SNR for C-MRC, we have resorted to using an approximation for the received SNR, which is independent of the underlying modulation scheme used. For our analysis
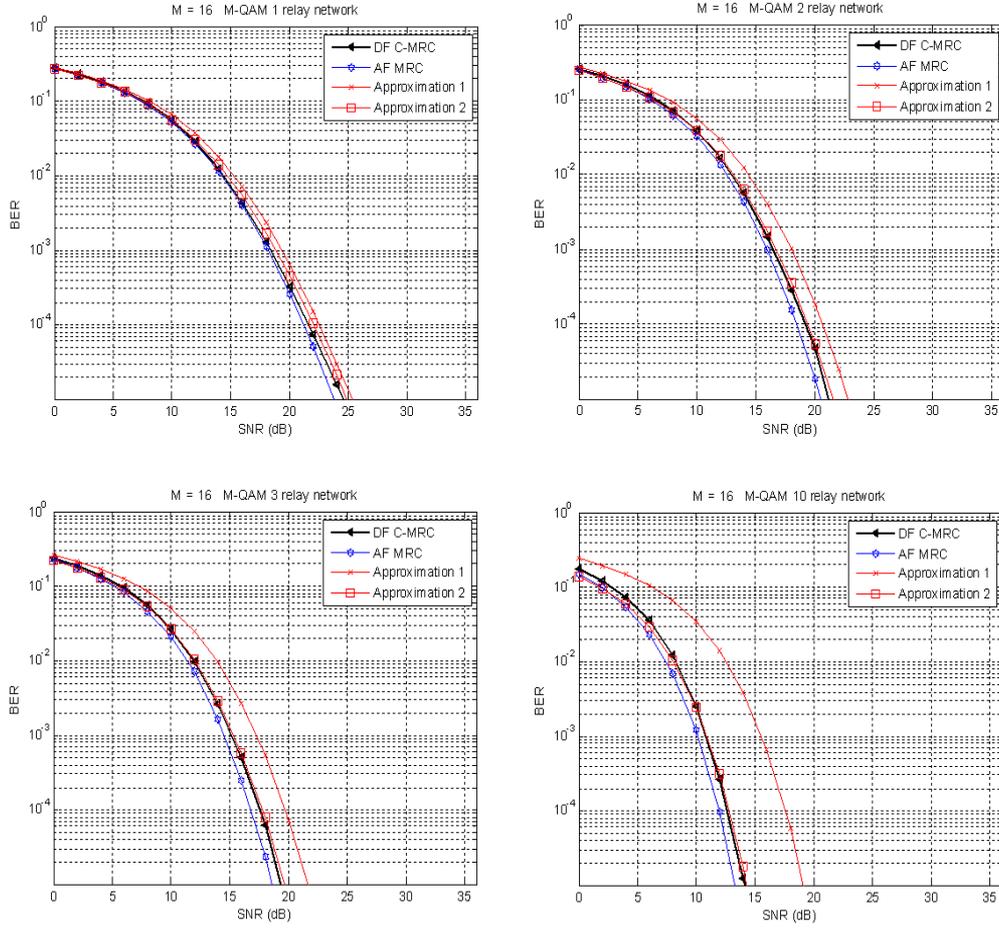
Figure 4.2: BER of 16-QAM for different numbers of cooperating relays with Nakagami-m fading, $m = 2$.

of AMQAM by using C-MRC, we have tested heuristic approximations of the received SNR via Monte Carlo simulations by using a trial-and-error approach. Two approximations for the received SNR are

$$\gamma_{\mathrm{ap}1} = \max(\gamma_{s,d}, \min(\gamma_{s,1}, \gamma_{1,d}), \dots, \min(\gamma_{s,N}, \gamma_{N,d})) \quad \text{and} \qquad (4.4)$$

$$\gamma_{\mathrm{ap}2} = \gamma_{s,d} + \sum_{i=1}^{N} 0.5 \min(\gamma_{s,i}, \gamma_{i,d}) \ . \qquad (4.5)$$

Simulations were carried out extensively in Rayleigh and Nakagami-m i.i.d. and non-i.i.d. fading environments with different numbers of cooperating DF relays. The decoding at the relays was performed by using ML detection, and the received signals were combined at the destination by using C-MRC according to (4.1), and

46

symbol detection was performed by using (4.3). Nakagami-m random variables were generated by using the method proposed in [65].

Fig. 4.1 shows the BER curves obtained for a cooperative network (non-adaptive constant rate) consisting of two DF relays under i.i.d. Nakagami-m fading with $m = 2$ for different modulation schemes. The BER curves show that $\gamma_{\mathrm{ap}\,2}$ given in (4.5) provides a very accurate approximation of the total received SNR at the destination under C-MRC. The performance of the two approximations for different numbers of cooperating relay nodes is illustrated in Fig. 4.2. As the number of relays increase, the accuracy of $\gamma_{\mathrm{ap}\,2}$ at the high SNR region increases while $\gamma_{\mathrm{ap}\,1}$ serves as a loose lower bound for the received SNR. The BER performance of the comparable AF relay network using MRC is also shown in Fig. 4.1 and 4.2. The BER performance of C-MRC scheme is only slightly less than that of the AF network employing MRC.

Fig. 4.3 depicts the outage probability associated with a two-DF relay cooperative network under 4-QAM transmission. The outage probability for C-MRC was derived by using the BER simulation results and considering a BER-based outage threshold of 0.01. A BER above this threshold was considered to result in an outage event. The corresponding theoretical C-MRC plot for outage probability was derived by using the approximation for received SNR $\gamma_{\mathrm{ap}\,2}$ and considering an equivalent outage SNR threshold of $7.33\,\mathrm{dB}$ (for 4-QAM, this threshold of 7.33 dB results in a BER of 0.01). Clearly, $\gamma_{\mathrm{ap}\,2}$ serves as a good approximation of the received SNR in terms of the outage probability.

From these BER and outage probability results, we take $\gamma_{\mathrm{ap}\,2}$ to be an accurate representation of the total received SNR with C-MRC.

4.3 Analysis of Adaptive M-QAM by using Cooperative MRC

The system model used for the analysis is similar to the model described in Chapter 2 , Section 2.3.2. However, in this analysis under C-MRC, we consider all DF relays to be participating in the decoding of signals as opposed to considering a subset
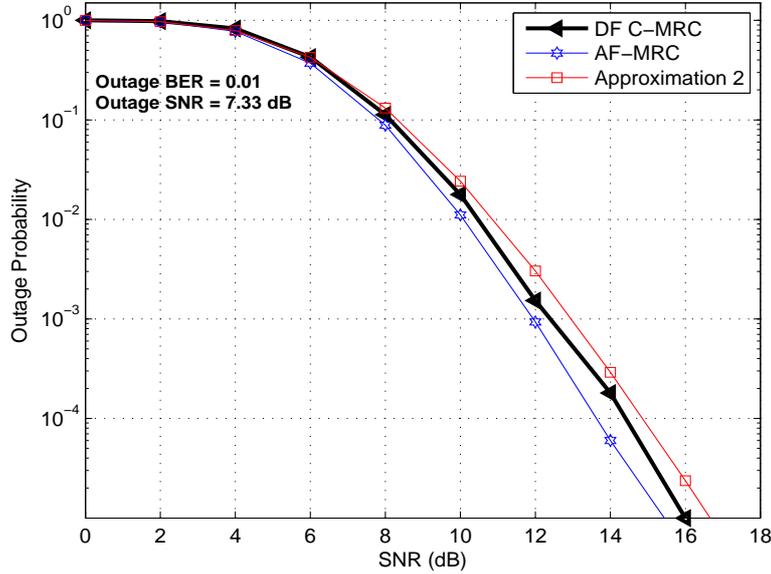
Figure 4.3: Outage probability for 4 - QAM, with i.i.d. Nakagami-m fading, $m = 2$, two relay network.

of relays which have a received SNR above a particular threshold. We use this approach because the diversity benefits received under C-MRC amidst decoding errors will maximize when the participation of the cooperating relays is increased. We consider i.i.d. Nakagami-m fading channels for the analysis. For simplicity, we use the rate adaptation scheme employing fixed switching levels as in Section 3.5.1.

For the analysis of C-MRC under the five-mode AMQAM, $\gamma_{\mathrm{ap\,2}}$ will be used to approximate the total received SNR at the destination. Therefore, the total received SNR at the destination is

$$\gamma_{\mathrm{tot}} \approx \gamma_{s,d} + \sum_{N}^{i=1} 0.5 \min(\gamma_{s,i}, \gamma_{i,d}) . \tag{4.6}$$

The PDF of the approximation for γ_{tot} is derived in Appendix B. By using PDF (B.7), the performance parameters described in Section 3.4 can be derived as follows.

Mode Selection Probability

This is the probability that the received SNR falls in the nth partition, resulting in the use of the nth mode for transmission at the transmitter. By using the PDF (B.7) in (3.1), the MSP can be derived as

$$
\delta_n = \frac{\Gamma^N(2m)}{2^{2N(m-1)}m^N\Gamma^{2N}(m)}\left\{\sum_{r=1}^{m}\Lambda_r\left[\frac{\Gamma\left(r,\frac{m\gamma_n}{\bar{\gamma}}\right)-\Gamma\left(r,\frac{m\gamma_{n+1}}{\bar{\gamma}}\right)}{\Gamma(r)}\right]\right.
$$
$$
\left.+\sum_{t=1}^{N(2m-1)}\Omega_t\left[\frac{\Gamma\left(t,\frac{4m\gamma_n}{\bar{\gamma}}\right)-\Gamma\left(t,\frac{4m\gamma_{n+1}}{\bar{\gamma}}\right)}{\Gamma(t)}\right]\right\}, \tag{4.7}
$$

where Λ_r and Ω_t are given in (B.5) and (B.6), respectively.

Outage Probability

When the SNR falls below the first switching level of γ_1, the transmitter selects the no transmit mode. The probability of the outage event caused by this selection can be found by using (3.4) as

$$
P_{out}=1-\frac{\Gamma^N(2m)}{2^{2N(m-1)}m^N\Gamma^{2N}(m)}\left\{\sum_{r=1}^{m}\Lambda_r\frac{\Gamma\left(r,\frac{m\gamma_1}{\bar{\gamma}}\right)}{\Gamma(r)}+\sum_{t=1}^{N(2m-1)}\Omega_t\frac{\Gamma\left(t,\frac{4m\gamma_1}{\bar{\gamma}}\right)}{\Gamma(t)}\right\}. \tag{4.8}
$$

Average Spectral Efficiency

The average spectral efficiency can be derived by substituting for δ_n in (3.7) by using (4.7):

$$
\frac{R}{B} = \frac{\Gamma^N(2m)}{2^{2N(m-1)}m^N\Gamma^{2N}(m)(N+1)}
$$
$$
\times\sum_{n=1}^{K-1}b_n\left\{\sum_{r=1}^{m}\Lambda_r\left[\frac{\Gamma\left(r,\frac{m\gamma_n}{\bar{\gamma}}\right)-\Gamma\left(r,\frac{m\gamma_{n+1}}{\bar{\gamma}}\right)}{\Gamma(r)}\right]\right.
$$
$$
\left.+\sum_{t=1}^{N(2m-1)}\Omega_t\left[\frac{\Gamma\left(t,\frac{4m\gamma_n}{\bar{\gamma}}\right)-\Gamma\left(t,\frac{4m\gamma_{n+1}}{\bar{\gamma}}\right)}{\Gamma(t)}\right]\right\}. \tag{4.9}
$$

Here, $\hat{N}$ in equation (3.7) is equal to N since all DF relays are cooperating to forward the source signal to the destination.

Average Bit Error Rate

The average BER can be calculated by using (3.10), where P_n, the mode-specific BER, is found to be (4.10) by using the equations (3.11), (3.15) and the PDF given in (B.7):

$$
P_n = \frac{\Gamma^N(2m)}{2^{2N(m-1)}\, m^N\, \Gamma^{2N}(m)} \Bigg[\sum_{r=1}^{m} \frac{\Lambda_r}{(r-1)!} \left(\frac{m}{\bar{\gamma}}\right)^r \sum_l A_l\, I_r(a_l, m/\bar{\gamma}, \gamma_n, \gamma_{n+1})
$$

$$
+ \sum_{t=1}^{N(2m-1)} \frac{\Omega_t}{(t-1)!} \left(\frac{4m}{\bar{\gamma}}\right)^t \sum_l A_l\, I_t(a_l, 4m/\bar{\gamma}, \gamma_n, \gamma_{n+1}) \Bigg] . \qquad (4.10)
$$

4.3.1 Numerical Results
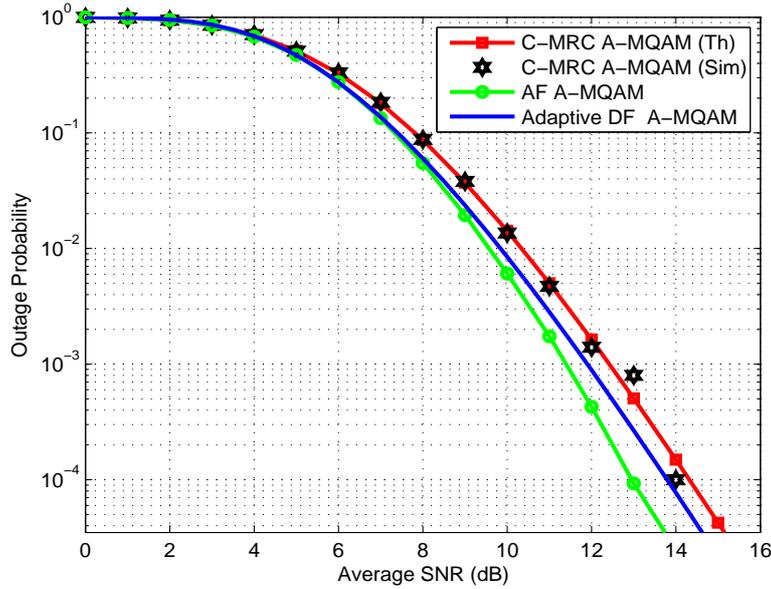
Figure 4.4: Outage probability, with i.i.d. Nakagami-m fading, $m = 2$, two relay network.

The results from the analytical equations derived from the approximation of the received SNR and the simulation results are compared. Simulations were performed on a system consisting of 2 DF cooperative relays where all channels are modeled as i.i.d. Nakagami-m with $m = 2$. Numerical results were also obtained for a comparable AF cooperative network and the adaptive DF cooperative network (with i.i.d. channels) discussed in Section 2.3.2, by using semi-analytical methods.

Fig. 4.4 shows the outage probability curves of the different systems. The outage performance under the C-MRC method is slightly less than the performances of the other systems. The best performance is attained with the AF relays with MRC diversity combining. The average spectral efficiency is depicted in Fig. 4.5. Both the C-MRC method and the AF MRC system perform equally well, while the adaptive DF system performs the best, where a performance gain of $2.5\,\text{dB}$ to $3\,\text{dB}$ in the average SNR is achieved for a given average spectral efficiency. For both the outage probability and average spectral efficiency, the simulation results and theoretical values of the C-MRC system match well. The outage probability and the average data rate depend on the criteria used for selecting the transmission modes at the transmitter. Since the approximation of the received SNR (4.5) was used as the basis for selecting the transmission modes, the theoretical values derived by using (4.5) should closely match the simulated values.
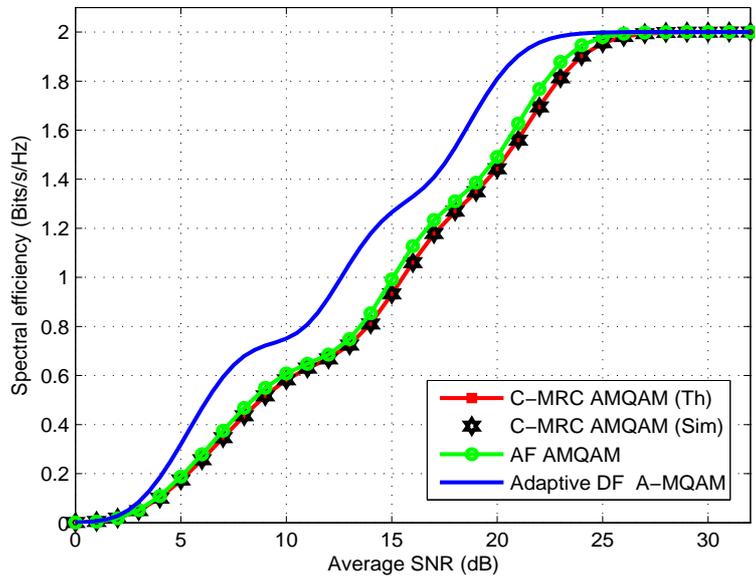

Figure 4.5: Average spectral efficiency, with i.i.d. Nakagami-m fading, $m = 2$, two relay network.

The average BER performance curves of the system using C-MRC are shown in Fig. 4.6. Except for the initial part of the BER curves, the simulation results stay below the BER QoS constraint of 1×10^{-3}. The theoretical curve gives a lower aver-

age BER than the simulation results. Furthermore, the gap between the theoretically approximated BER and the simulated BER has increased for rate adaptive transmission, unlike the case for the fixed rate transmission discussed in Subsection 4.2.2. However, for non-adaptive fixed rate transmission, the average BER is obtained by averaging the instantaneous BER values over all possible channel conditions for a particular fixed modulation scheme, but in the rate adaptive scheme simulated here, the instantaneous BER corresponding to the higher modulation schemes will always correspond to favorable channel conditions while the instantaneous BER of the lower modulation schemes will always relate to poor channel conditions, due to the switching levels employed. Hence, we can see that the accuracy of the approximation of the total received SNR under C-MRC decreased when the rate adaptive transmission was considered. This conclusion is further supported by the observation that for higher SNR values, above 25 dB, the simulation and theoretical curves overlap and show a good match, where the transmitter selects the highest mode with a very high probability (a very low probability of switching to lower modes at high average SNR values). In the high SNR region, since the transmitter operation is similar to that of a non-adaptive fixed rate transmitter, the simulation and theoretical results are in accordance, as opposed to the results in the lower SNR regions where adaptation is employed. The average BER curve obtained with 64-QAM by using C-MRC is also given in the figure. For high SNR values, all curves show the same diversity order. Fig. 4.7 shows a comparison of the BER performance under fixed switching levels of the different types of cooperative networks discussed so far.

4.4   Summary

This chapter considered the effect of the decoding errors at the cooperating relays on the rate adaptive transmission used in cooperative DF networks. These decoding errors are accounted for in the final result observed at the destination receiver through the use of cooperative demodulation and symbol detection. The different cooperative demodulation, detection, and diversity-combining techniques available
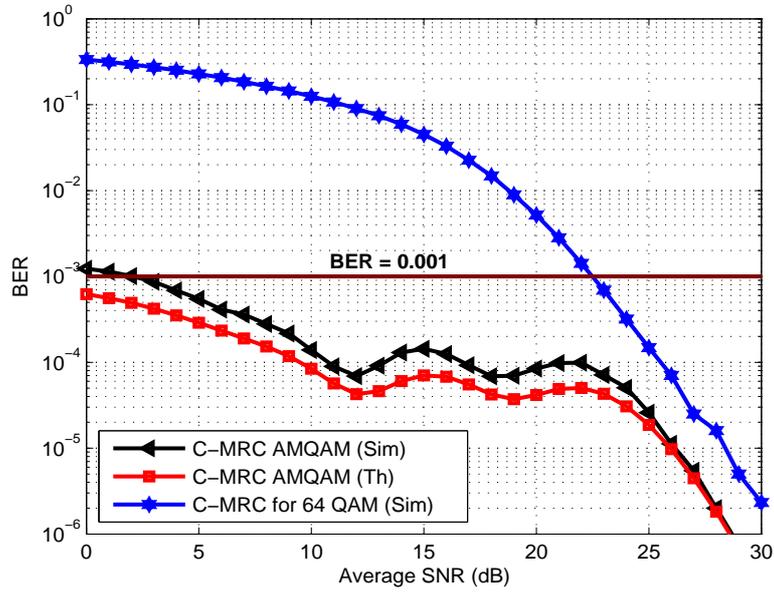
Figure 4.6: Average BER for system using C-MRC, with i.i.d. Nakagami-m fading, $m = 2$, two relay network.
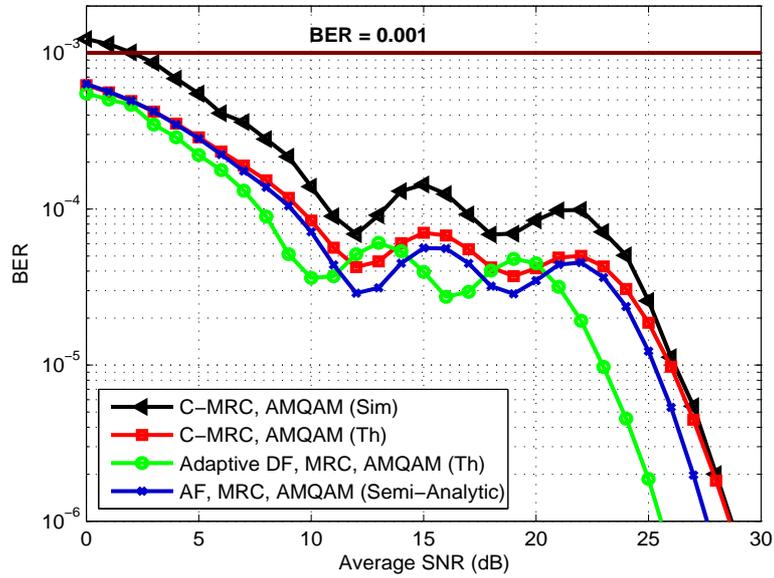
Figure 4.7: Comparison of Average BER in different cooperative systems with i.i.d. Nakagami-m fading, $m = 2$, two relay network.

in the literature were discussed, and C-MRC was chosen for our analysis due to its simplicity and near-ML performance. A heuristic approximation of the received

SNR was obtained through simulations. The results show that the rate adaptive system with C-MRC maintained the desired QoS constraint. The performance of other cooperative systems were compared with those of the C-MRC system. When compared to the Adaptive DF system discussed in Chapter 3 where error-free decoding was assumed (with a decoding SNR threshold), the system under C-MRC showed a reduction in average spectral efficiency for a given average SNR due to the presence of decoding errors at the relays.

Chapter 5

Conclusions

This thesis focused mainly on DF cooperative networks with rate adaptive transmission. The purpose of this research was to observe how the integration cooperative diversity and adaptive transmission affects system performance. As stated in Chapter 1, both of these techniques are used in either combating the detrimental effects of the wireless channel or in exploiting the inherent nature of the channel, in order to improve the overall system performance.

In Chapter 2, analytical expressions for the channel capacity of DF and AF cooperative networks were derived. By using these expressions, the channel capacity for the rate adaptive transmission with a cooperative network was derived. Our results show that DF cooperative networks achieved a bigger capacity than that of AF cooperative networks. However, these favorable results were obtained under the ideal assumption that the symbol decoding at the relays is error-free.

In Chapter 3, a constant power rate adaptive transmission scheme was implemented by using a discrete set of transmission modes comprised of square M-QAM constellations under a BER QoS constraint. The proposed DF cooperative system was tested by using this rate adaptive scheme. The system performance was investigated under two types of switching level assignments. By comparing the theoretical values and simulation results from the performance metrics (outage probability, mode selection probabilities, average spectral efficiency, average BER), it was established that the optimal switching level assignment provided a better performance than that of the fixed switching assignment; e.g., gains of 2 - 3 dB in the SNR were

observed for a given average spectral efficiency. However, fixed switching proved to be a simple method for assigning transmission modes and resulted in maintaining a conservative QoS level.

The effect of the errors in symbol decoding at the cooperative relays was investigated in Chapter 4. Different cooperative demodulation and detection techniques were discussed to account for the errors at relays. Cooperative-MRC was used to analyze the performance of the cooperative network under rate adaptation due to its simplicity of implementation and near-maximal likelihood performance. Due to the complications involved in deriving an exact expression for the total received SNR at the destination receiver by using the C-MRC technique, an accurate approximation of the received SNR was proposed. This approximation provided an accurate match to the simulation results obtained for the BER and outage probability of the fixed rate cooperative DF networks. However, the accuracy decreased when this approximation was used with rate adaptive systems. The performance of the DF cooperative system under C-MRC was almost as good as that under a comparable AF cooperative system. The decoding errors at the DF relays reduced the system performance when compared with the performance of the ideal DF cooperative network used in Chapter 3. A reduction of 2.5 to 3 dB was observed in the average SNR for a given average spectral efficiency due to the presence of the decoding errors at the relays.

5.1   Future Research Directions

This thesis work provides a foundation for further research on several interesting topics that were not addressed in our analysis of adaptive transmission with cooperative networks. In the analysis of the adaptive system, it was assumed that the feedback channel is ideal, with zero delay and zero error probability. The effect of non-zero delay and non-zero error probability is to reduce the throughput of the adaptive system. Further performance analysis is required to quantify the impact of the feedback channel imperfections on the system performance. The cooperative demodulation and detection of signals and the estimation of the total received SNR

at the destination relies mainly on the accuracy of the CSI estimation. Therefore, the effect of the CSI estimation errors on the overall system performance of the cooperative network also requires further research.

Bibliography

[1] L. Eastwood, S. Migaldi, Q. Xie, and V. Gupta, "Mobility using IEEE 802.21 in a heterogeneous IEEE 802.16/802.11-based, IMT-advanced (4g) network," *IEEE Wireless Communications*, vol. 15, no. 2, pp. 26–34, Apr. 2008.

[2] S. Ahmadi, "An overview of next-generation mobile WiMAX technology - [WiMAX update]," *IEEE Communications Magazine*, vol. 47, no. 6, pp. 84–98, Jun. 2009.

[3] D. Astely, E. Dahlman, A. Furuskar, Y. Jading, M. Lindstrom, and S. Parkvall, "LTE: the evolution of mobile broadband - [LTE part II: 3GPP release 8]," *IEEE Communications Magazine*, vol. 47, no. 4, pp. 44–51, Apr. 2009.

[4] A. Goldsmith, *Wireless Communications*. New York, NY, USA: Cambridge University Press, 2005.

[5] Y. G. Li and G. L. Stuber, *Orthogonal Frequency Division Multiplexing for Wireless Communications*. Springer, 2006.

[6] E. Biglieri, R. Calderbank, A. Constantinides, A. Goldsmith, A. Paulraj, and H. Poor, *MIMO Wireless Communications*. Cambridge University Press, 2007.

[7] R. van Nee, G. Awater, M. Morikura, H. Takanashi, M. Webster, and K. W. Halford, "New high-rate wireless LAN standards," *IEEE Commun. Mag.*, vol. 37, no. 12, pp. 82–88, Dec. 1999.

[8] M. Tran, A. Doufexi, and A. Nix, "Mobile WiMAX MIMO performance analysis: Downlink and uplink," in *Personal, Indoor and Mobile Radio Communications, 2008. PIMRC 2008. IEEE 19th International Symposium on*, Cannes, Sep. 2008, pp. 1–5.

[9] W. Xiang, P. Richardson, and J. Guo, "Introduction and preliminary experimental results of wireless access for vehicular environments (WAVE) systems," in *Mobile and Ubiquitous Systems - Workshops, 2006. 3rd Annual International Conference on*, San Jose, CA, Jul. 2006, pp. 1–8.

[10] J. N. Laneman, D. N. C. Tse, and G. W. Wornell, "Cooperative diversity in wireless networks: Efficient protocols and outage behavior," *IEEE Transactions on Information Theory*, vol. 50, pp. 3062–3080, Dec. 2004.

[11] M. O. Hasna, "On the capacity of cooperative diversity systems with adaptive modulation," in *Wireless and Optical Communications Networks, 2005. WOCN 2005. Second IFIP International Conference on*, Mar. 2005, pp. 432–436.

[12] K. S. Hwang, Y. Ko, and M.-S. Alouini, "Performance analysis of opportunistic incremental relaying with adaptive modulation," in *Proc. IEEE International Symposium on Wireless Pervasive Computing 2008*, May 2008.

[13] T. Nechiporenko, K. T. Phan, C. Tellambura, and H. H. Nguyen, "On the capacity of Rayleigh fading cooperative systems under adaptive transmission," *IEEE Transactions on Wireless Communications*, vol. 8, no. 4, pp. 1626–1631, Apr. 2009.

[14] ——, "Performance analysis of adaptive M-QAM for Rayleigh fading cooperative systems," in *Proc. IEEE International Conference on Communications (ICC)*, May 2008, pp. 3393–3399.

[15] T. Nechiporenko, P. Kalansuriya, and C. Tellambura, "Performance of optimum switching adaptive M-QAM for amplify-and-forward relays," *IEEE Transactions on Vehicular Technology*, vol. 58, no. 5, pp. 2258–2268, Jun. 2009.

[16] D. Tse and P. Viswanath, *Fundamentals of Wireless Communication*. New York, NY, USA: Cambridge University Press, 2005.

[17] A. Sendonaris, E. Erkip, and B. Aazhang, "Increasing uplink capacity via user cooperation diversity," in *Information Theory, 1998. Proceedings. 1998 IEEE International Symposium on*, Cambridge, MA, USA, Aug. 1998.

[18] A. Nosratinia, T. E. Hunter, and A. Hedayat, "Cooperative communication in wireless networks," *IEEE Communications Magazine*, vol. 42, no. 10, pp. 74–80, Oct. 2004.

[19] Y. Liu, R. Hoshyar, X. Yang, and R. Tafazolli, "Integrated radio resource allocation for multihop cellular networks with fixed relay stations," *IEEE Journals on Selected Areas in Communications*, vol. 24, no. 11, pp. 2137–2146, Nov. 2006.

[20] H. Nourizadeh, S. Nourizadeh, and R. Tafazolli, "Impact of the inter-relay handoff on the relaying system performance," in *Vehicular Technology Conference, 2006. VTC-2006 Fall. 2006 IEEE 64th*, Montreal, Que., Sep. 2006, pp. 1–5.

[21] A. Imran and R. Tafazolli, "Evaluation and comparison of capacities and costs of multihop cellular networks," in *Telecommunications, 2009. ICT '09. International Conference on*, Marrakech, May 2009, pp. 160–165.

[22] T. Cover and A. E. Gamal, "Capacity theorems for the relay channel," *IEEE Transactions on Information Theory*, vol. 25, no. 5, pp. 572–584, Sep. 1979.

[23] C. Casetti, C. F. Chiasserini, and L. Previtera, "Fair relaying and cooperation in multi-rate 802.11 networks," in *Vehicular Technology Conference, 2005. VTC 2005-Spring. 2005 IEEE 61st*, vol. 3, May/Jun. 2005, pp. 2033–2036.

[24] L. Dai, W. Chen, L. J. Cimini Jr., and K. B. Letaief, "Fairness improves throughput in energy-constrained cooperative ad-hoc networks," *IEEE Transactions on Wireless Communications*, vol. 8, no. 7, pp. 3679–3691, Jul. 2009.

[25] S. Vishwanath, S. Jafar, and S. Sandhu, "Half-duplex relays: cooperative communication strategies and outer bounds," in *Wireless Networks, Communications and Mobile Computing, 2005 International Conference on*, vol. 2, Jun. 2005, pp. 1455–1459.

[26] T. Riihonen, R. Wichman, and J. Hamalainen, "Co-phasing full-duplex relay link with non-ideal feedback information," in *Wireless Communication Systems. 2008. ISWCS '08. IEEE International Symposium on*, Oct. 2008, pp. 263–267.

[27] R. Price, "Error probabilities for adaptive multichannel reception of binary signals," *IRE Transactions on Information Theory*, vol. 8, no. 5, pp. 305–316, Sep. 1962.

[28] J. Hayes, "Adaptive feedback communications," *IEEE Transactions on Communications Technology [legacy, pre - 1988]*, vol. 16, no. 1, pp. 29–34, Feb. 1968.

[29] A. Svensson, "An introduction to adaptive QAM modulation schemes for known and predicted channels," *Proc. IEEE*, vol. 95, no. 12, pp. 2322–2336, Dec. 2007.

[30] H. Zhang, S. Wei, G. Ananthaswamy, and D. L. Goeckel, "Adaptive signaling based on statistical characterizations of outdated feedback in wireless communications," *Proc. IEEE*, vol. 95, no. 12, pp. 2337–2353, Dec. 2007.

[31] X. Qiu and J. Chuang, "Link adaptation in wireless data networks for throughput maximization under retransmissions," in *Communications, 1999. ICC '99. 1999 IEEE International Conference on*, vol. 2, Vancouver, BC, Jun. 1999, pp. 1272–1277.

[32] S. Nanda, K. Balachandran, and S. Kumar, "Adaptation techniques in wireless packet data services," *IEEE Communications Magazine*, vol. 38, no. 1, pp. 54–64, Jan. 2000.

[33] L. Caponi, F. Chiti, and R. Fantacci, "Performance evaluation of a link adaptation technique for high speed wireless communication systems," *IEEE Transactions on Wireless Communications*, vol. 6, no. 12, pp. 4568–4575, Dec. 2007.

[34] M.-S. Alouini and A. J. Goldsmith, "Capacity of Rayleigh fading channels under different adaptive transmission and diversity-combining techniques," *IEEE Transactions on Vehicular Technology*, vol. 48, pp. 1165–1181, Jul. 1999.

[35] A. J. Goldsmith and P. P. Varaiya, "Capacity of fading channels with channel side information," *IEEE Transactions on Information Theory*, vol. 43, pp. 1986–1992, Nov. 1997.

[36] A. J. Goldsmith and S.-G. Chua, "Variable-rate variable-power MQAM for fading channels," *IEEE Transactions on Communications*, vol. 45, pp. 1218–1230, Oct. 1997.

[37] P. Kalansuriya and C. Tellambura, "Capacity analysis of a decode-and-forward cooperative network under adaptive transmission," in *Electrical and Computer Engineering, 2009. CCECE '09. Canadian Conference on*, St. John's, NL, Canada, May 2009, pp. 298–303.

[38] ——, "Performance analysis of decode-and-forward relay network under adaptive M-QAM," in *Proc. IEEE International Conference on Communications (ICC)*, 2009.

[39] ——, "Rate Adaptive Transmission Under Cooperative Demodulation," *submitted to IEEE Transactions on Wireless Communications*.

[40] M. Nakagami, "The m-Distribution, a general formula of intensity of rapid fading," in *Proc. Statistical Methods in Radio Wave Propagation*, W. G. Hoffman, Ed. Elmsford, NY: Permagon Press, 1960, pp. 3–36.

[41] H. Suzuki, "A statistical model for urban radio propogation," *IEEE Transactions on Communications*, vol. 25, no. 7, pp. 673–680, Jul. 1977.

[42] A. U. Sheikh, M. Abdi, and M. Handforth, "Indoor mobile radio channel at 946 MHz: Measurements and modeling," in *Vehicular Technology Conference, 1993 IEEE 43rd*, Secaucus, NJ, May 1993, pp. 73–76.

[43] M. K. Simon and M.-S. Alouini, *Digital Communication over Fading Channels*. New Jersey NJ: John Wiley & Sons, Inc, 2005.

[44] G. L. Stuber, *Principles of Mobile Communications*. KLUWER ACADEMIC PUBLISHERS, 2002.

[45] P. A. Anghel and M. Kaveh, "Exact symbol error probability of a cooperative network in a Rayleigh-fading environment," *IEEE Transactions on Wireless Communications*, vol. 3, pp. 1416–1421, Sep. 2004.

[46] S. Ikki and M. H. Ahmed, "Performance analysis of cooperative diversity wireless networks over Nakagami-*m* fading channel," *IEEE Communications Letters*, vol. 11, pp. 334–336, Jul. 2007.

[47] K. S. Hwang, Y. Ko, and M.-S. Alouini, "Performance analysis of incremental opportunistic relaying over identically and non-identically distributed cooperative paths," *IEEE Transactions on Wireless Communications*, vol. 8, pp. 1953–1961, Apr. 2009.

[48] S. Ikki and M. Ahmed, "Performance of decode-and-forward cooperative diversity networks over nakagami-m fading channels," *Global Telecommunications Conference, 2007. GLOBECOM '07. IEEE*, pp. 4328–4333, Nov. 2007.

[49] N. C. Sagias, F. I. Lazarakis, G. S. Tombras, and C. K. Datsikas, "Outage analysis of decode-and-forward relaying over Nakagami-m fading channels," *IEEE Signal Processing Letters*, vol. 15, pp. 41–44, 2008.

[50] C. T. K. Ng and A. J. Goldsmith, "Capacity and power allocation for transmitter and receiver cooperation in fading channels," in *Communications, 2006. ICC '06. IEEE International Conference on*, vol. 8, Jun. 2006, pp. 3741–3746.

[51] A. Seyoum and N. C. Beaulieu, "Semi-analytical simulation for evaluation of block error rates onfading channels," in *Global Telecommunications Conference, 1996. GLOBECOM '96. 'Communications: The Key to Global Prosperity*, vol. 2, London, UK, Nov. 1996, pp. 1268–1272.

[52] B. Choi and L. Hanzo, "Optimum mode-switching-assisted constant-power single- and multicarrier adaptive modulation," *IEEE Transactions on Vehicular Technology*, vol. 52, no. 3, pp. 536–560, May 2003.

[53] A. R. Leyman, X. Liu, H. K. Garg, and Y. Xin, "Automatic classification of imperfect QAM constellation using radon transform," in *Communications, 2007. ICC '07. IEEE International Conference on*, Glasgow, Jun. 2007, pp. 2635–2640.

[54] L. De Vito, S. Rapuano, and M. Villanacci, "An improved method for the automatic digital modulation classification," in *Instrumentation and Measurement Technology Conference Proceedings, 2008. IMTC 2008. IEEE*, Victoria, BC, May 2008, pp. 1441–1446.

[55] A. Doufexi, S. Armour, M. Butler, A. Nix, D. Bull, J. McGeehan, and P. Karlsson, "A comparison of the HIPERLAN/2 and IEEE 802.11a wireless LAN standards," *IEEE Commun. Mag.*, vol. 40, no. 5, pp. 172–180, May 2002.

[56] Q. Liu, S. Zhou, and G. B. Giannakis, "Cross-layer combining of adaptive modulation and coding with truncated ARQ over wireless links," *IEEE Transactions on Wireless Communications*, vol. 3, no. 5, pp. 1746–1755, Sep. 2004.

[57] B. Can, H. Yanikomeroglu, F. A. Onat, E. De Carvalho, and H. Yomo, "PHY 02-2 - efficient cooperative diversity schemes and radio resource allocation for IEEE 802.16j," in *Wireless Communications and Networking Conference, 2008. WCNC 2008. IEEE*, Las Vegas, NV, Mar./Apr. 2008, pp. 36–41.

[58] M.-S. Alouini and A. J. Goldsmith, "Adaptive modulation over Nakagami fading channels," *Wireless Personal Communications*, vol. 13, pp. 119–143, 2000.

[59] J. Adeane, M. R. D. Rodrigues, and I. J. Wassell, "Characterisation of the performance of cooperative networks in ricean fading channels," in *12th International Conference on Telecommunications (ICT 2005)*, May 2005.

[60] A. Sendonaris, E. Erkip, and B. Aazhang, "User cooperation diversity part II: implementation aspects and performance analysis," *IEEE Transactions on Communications*, vol. 51, pp. 1939–1948, Nov. 2003.

[61] D. Chen and J. N. Laneman, "Modulation and demodulation for cooperative diversity in wireless systems," *IEEE Transactions on Wireless Communications*, vol. 5, no. 7, pp. 1785–1794, Jul. 2006.

[62] T. Wang, A. Cano, G. B. Giannakis, and J. N. Laneman, "High-performance cooperative demodulation with decode-and-forward relays," *IEEE Transactions on Communications*, vol. 55, no. 7, pp. 1427–1438, Jul. 2007.

[63] Z. Yi and I.-M. Kim, "Decode-and-forward cooperative networks with relay selection," in *Vehicular Technology Conference, 2007. VTC-2007 Fall. 2007 IEEE 66th*, Sep./Oct. 2007, pp. 1167–1171.

[64] T. Wang, A. Cano, and G. B. Giannakis, "Efficient Demodulation in Cooperative Schemes Using Decode-and-Forward Relays," in *Signals, Systems and Computers, 2005. Conference Record of the Thirty-Ninth Asilomar Conference on*, Oct./Nov. 2005, pp. 1051–1055.

[65] N. C. Beaulieu and C. Cheng, "Efficient Nakagami-m Fading channel Simulation," *IEEE Transactions on Vehicular Technology*, vol. 54, no. 2, pp. 413–424, Mar. 2005.

[66] I. Gradshteyn and I. Ryzhik, *Table of Integrals, Series, and Products, Sixth Edition*. Academic Press, 2000.

Appendix A

Derivation of PDF of the received SNR for AF Cooperative Network

A.1 PDF for AF Relay Network with i.i.d. Nakagami-m Fading

Eq. (2.7) gives the upper bound of the total received SNR at the destination γ_{ub} . Since since γ_i and $\gamma_{s,d}$ are independent, the MGF of γ_{ub} can be expressed as

$$M_{\gamma_{ub}}(s) = M_{\gamma_{s,d}}(s) \prod_{i=1}^{N} M_{\gamma_i}(s) .$$

(A.1)

Since $\gamma_{s,d}$ is Gamma distributed with shape parameter m and scale parameter $\bar{\gamma}/m$, $M_{\gamma_{s,d}}(s)$ can be written as

$$M_{\gamma_{s,d}}(s) = (1 + \bar{\gamma}/ms)^{-m} .$$

(A.2)

It is shown in [46] that for i.i.d. Nakagami-m fading, the MGF for the i-th branch can be written as

$$M_{\gamma_i}(s) = \left(\frac{m}{\bar{\gamma}}\right)^{2m} \frac{\Gamma(2m)}{m\Gamma^2(m)} \frac{2}{(2m/\bar{\gamma} + s)^{2m}} \times {}_2F_1\left(1, 2m; m+1; \frac{m/\bar{\gamma} + s}{2m/\bar{\gamma} + s}\right) ,$$

(A.3)

where ${}_2F_1(\alpha, \beta; \gamma; z)$ is the hypergeometric function defined in [66, 9.100].

By using the transform of [66, 9.131]

$${}_2F_1\left(1, 2m; m+1; \frac{m/\bar{\gamma} + s}{2m/\bar{\gamma} + s}\right) = \frac{2m/\bar{\gamma} + s}{m/\bar{\gamma}} {}_2F_1\left(1, 1-m; m+1; -\frac{m/\bar{\gamma} + s}{m/\bar{\gamma}}\right)$$

(A.4)

64

and by using the properties of [66, 9.100] for $\beta < 0$, the hypergeometric series can be written as

$$
{}_2F_1\left(1, 1-m; m+1; -\frac{m/\bar\gamma + s}{m/\bar\gamma}\right) = \sum_{k=0}^{m-1} a_k \left(-\frac{m/\bar\gamma + s}{m/\bar\gamma}\right)^k, \tag{A.5}
$$

where a_k are the hypergeometric coefficients give as

$$
\begin{array}{rcl}
a_0 & = & 1 \\
a_k & = & \frac{(1-m)(2-m)...(k-m)}{(m+1)(m+2)...(m+k)} .
\end{array} \tag{A.6}
$$

By substituting (A.5) into (A.4) and then into (A.3), the MGF can be written as

$$
M_{\gamma_i}(s) = \left(\frac{m}{\bar\gamma}\right)^{2m} \frac{\Gamma(2m)}{m\Gamma^2(m)} \frac{2}{(2m/\bar\gamma + s)^{2m}} \frac{2m/\bar\gamma + s}{m/\bar\gamma} \sum_{k=0}^{m-1} a_k \left(-\frac{m/\bar\gamma + s}{m/\bar\gamma}\right)^k. \tag{A.7}
$$

By using (A.1), the MGF of the effective SNR is

$$
M_{\gamma_{ub}}(s) = \left[1 + \frac{\bar\gamma}{m}s\right]^{-m} \left[\left(\frac{m}{\bar\gamma}\right)^{2m-1} \frac{\Gamma(2m)}{m\Gamma^2(m)} \frac{2}{(2m/\bar\gamma + s)^{2m-1}} \sum_{k=0}^{m-1} a_k \left(-\frac{m/\bar\gamma + s}{m/\bar\gamma}\right)^k\right]^N. \tag{A.8}
$$

By re-arranging (A.8) and simplifying, the MGF can be written as

$$
M_{\gamma_{ub}}(s) = \frac{\Gamma^N(2m)(0.5)^{2N(m-1)}}{m^N\Gamma^{2N}(m)\left[1 + \frac{\bar\gamma}{m}s\right]^m\left[1 + \frac{\bar\gamma}{2m}s\right]^{N(2m-1)}} \left[\sum_{k=0}^{m-1} a_k(-1)^k\left(1 + \frac{\bar\gamma}{m}s\right)^k\right]^N. \tag{A.9}
$$

First, the numerator can be written as follows by using binomial expansion:

$$
\begin{array}{rcl}
\left[\displaystyle\sum_{k=0}^{m-1} a_k(-1)^k\left(1 + \frac{\bar\gamma}{m}s\right)^k\right]^N & = & \left[\displaystyle\sum_{k=0}^{m-1} a_k(-1)^k \sum_{l=0}^{k}\binom{k}{l}\left(\frac{\bar\gamma}{m}s\right)^l\right]^N \\[4mm]
& = & \left[\displaystyle\sum_{j=0}^{m-1} u_j\left(\frac{\bar\gamma}{m}s\right)^j\right]^N,
\end{array} \tag{A.10}
$$

where u_j are defined as

$$
u_j = \sum_{i=j}^{m-1} a_i(-1)^i\binom{i}{j}. \tag{A.11}
$$

By using a power series raised to power [66, 0.314]

$$
\left[\sum_{j=0}^{m-1} u_j\left(\frac{\bar\gamma}{m}s\right)^j\right]^N = \sum_{j=0}^{N(m-1)} v_j\left(\frac{\bar\gamma}{m}s\right)^j, \tag{A.12}
$$

where

$$
\begin{aligned}
v_0 &= u_0^N \\
v_j &= \frac{1}{j u_0} \sum_{r=1}^{j} (rN - j + r) u_r v_{j-r} \ ,
\end{aligned}
\tag{A.13}
$$

and by substituting back into the MGF of (A.9), we get

$$
M_{\gamma_{ub}}(s) = (0.5)^{2N(m-1)} \frac{\Gamma^N(2m)}{m^N \Gamma^{2N}(m)} \frac{\sum_{j=0}^{N(m-1)} v_j(\frac{\bar{\gamma}}{m}s)^j}{\left[1 + \frac{\bar{\gamma}}{m}s\right]^m \left[1 + \frac{\bar{\gamma}}{2m}s\right]^{N(2m-1)}} \ .
\tag{A.14}
$$

By using partial fractions, (A.14) can be rewritten as

$$
M_{\gamma_{ub}}(s) = (0.5)^{2N(m-1)} \frac{\Gamma^N(2m)}{m^N \Gamma^{2N}(m)} \left[\sum_{r=1}^{m} \Delta_r \left(1 + \frac{\bar{\gamma}}{m}s\right)^{-r} + \sum_{t=1}^{N(2m-1)} \Psi_t \left(1 + \frac{\bar{\gamma}}{2m}s\right)^{-t} \right],
\tag{A.15}
$$

where

$$
\Delta_r = \frac{(\frac{\bar{\gamma}}{m})^{(r-m)}}{(m-r)!} \frac{\partial^{m-r}}{\partial s^{m-r}} \left[\sum_{j=0}^{N(m-1)} v_j \left(\frac{\bar{\gamma}}{m}s\right)^j \left[1 + \frac{\bar{\gamma}}{2m}s\right]^{-N(2m-1)} \right]_{s=-m/\bar{\gamma}}
\tag{A.16}
$$

and

$$
\Psi_t = \frac{(\frac{\bar{\gamma}}{2m})^{(t-N(2m-1))}}{(N(2m-1)-t)!} \frac{\partial^{N(2m-1)-t}}{\partial s^{N(2m-1)-t}} \left[\sum_{j=0}^{N(m-1)} v_j \left(\frac{\bar{\gamma}}{m}s\right)^j \left[1 + \frac{\bar{\gamma}}{m}s\right]^{-m} \right]_{s=-2m/\bar{\gamma}} .
\tag{A.17}
$$

By taking the inverse Laplace transform of $M_{\gamma_{ub}}(s)$ in (A.15) and using the fact that $\mathcal{L}^{-1}\{(1 + as)^{-k}\} = \frac{1}{(k-1)! a^k} x^{k-1} e^{-\frac{x}{a}}$, the PDF of γ_{ub} is computed as follows:

$$
\begin{aligned}
f_{\gamma_{ub}}(\gamma) &= \frac{\Gamma^N(2m)}{m^N \Gamma^{2N}(m) 2^{2N(m-1)}} \Bigg[\sum_{r=1}^{m} \frac{\Delta_r}{(r-1)!} \left(\frac{m}{\bar{\gamma}}\right)^r \gamma^{r-1} e^{\frac{-\gamma m}{\bar{\gamma}}} \\
&\quad + \sum_{t=1}^{N(2m-1)} \frac{\Psi_t}{(t-1)!} \left(\frac{2m}{\bar{\gamma}}\right)^t \gamma^{t-1} e^{\frac{-\gamma 2m}{\bar{\gamma}}} \Bigg].
\end{aligned}
\tag{A.18}
$$

A.2 PDF for AF Relay Network with non-i.i.d. Nakagami-m Fading

The PDF can be found by using a similar technique to that used in the case of i.i.d. In [46], for non-i.i.d. Nakagami-m fading, the MGF for the i-th branch is written

as

$$M_{\gamma_i}(s) = \left(\frac{m_{s,i}}{\bar{\gamma}_{i,d}}\right)^{m_{s,i}} \left(\frac{m_{i,d}}{\bar{\gamma}_{i,d}}\right)^{m_{i,d}} \frac{\Gamma(m_{s,i}+m_{i,d})}{\Gamma(m_{s,i})\Gamma(m_{s,i})} \frac{1}{(m_{s,i}/\bar{\gamma}_{s,i}+m_{i,d}/\bar{\gamma}_{i,d}+s)^{m_{s,i}+m_{i,d}}}$$
$$\times \left[\frac{1}{m_{s,i}} {}_2F_1\left(1, m_{s,i}+m_{i,d}; m_{s,i}+1; \frac{m_{s,i}/\bar{\gamma}_{s,i}+s}{m_{s,i}/\bar{\gamma}_{s,i}+m_{i,d}/\bar{\gamma}_{i,d}+s}\right) \right.$$
$$\left. + \frac{1}{m_{i,d}} {}_2F_1\left(1, m_{s,i}+m_{i,d}; m_{i,d}+1; \frac{m_{i,d}/\bar{\gamma}_{i,d}+s}{m_{s,i}/\bar{\gamma}_{s,i}+m_{i,d}/\bar{\gamma}_{i,d}+s}\right) \right].$$

(A.19)

By using the transform [66, 9.131], the first hypergeometric function in (A.19) can be written as

$${}_2F_1\left(1, m_{s,i}+m_{i,d}; m_{s,i}+1; \frac{m_{s,i}/\bar{\gamma}_{s,i}+s}{m_{s,i}/\bar{\gamma}_{s,i}+m_{i,d}/\bar{\gamma}_{i,d}+s}\right) =$$
$$\left[\frac{m_{s,i}/\bar{\gamma}_{s,i}+m_{i,d}/\bar{\gamma}_{i,d}+s}{m_{i,d}/\bar{\gamma}_{i,d}}\right] {}_2F_1\left(1, 1-m_{i,d}; m_{s,i}+1; -\frac{m_{s,i}/\bar{\gamma}_{s,i}+s}{m_{i,d}/\bar{\gamma}_{i,d}}\right).$$

(A.20)

By using the properties of ${}_2F_1(\alpha, \beta; \gamma; z)$ [66, 9.100] for $\beta < 0$, the hypergeometric series can be written as

$${}_2F_1\left(1, 1-m_{i,d}; m_{s,i}+1; -\frac{m_{s,i}/\bar{\gamma}_{s,i}+s}{m_{i,d}/\bar{\gamma}_{i,d}}\right) = \sum_{k=0}^{m_{i,d}-1} a_k(-1)^k \left(\frac{m_{s,i}/\bar{\gamma}_{s,i}+s}{m_{i,d}/\bar{\gamma}_{i,d}}\right)^k$$
$$= \sum_{k=0}^{m_{i,d}-1} a_k(-1)^k \left(\frac{m_{s,i}\bar{\gamma}_{i,d}}{m_{i,d}\bar{\gamma}_{s,i}}\right)^k$$
$$\times \left(1+\frac{\bar{\gamma}_{s,i}}{m_{s,i}}s\right)^k$$
$$= \sum_{j=0}^{m_{i,d}-1} \mu_j \left(\frac{\bar{\gamma}_{s,i}}{m_{s,i}}s\right)^j, \qquad \text{(A.21)}$$

where a_k are the hypergeometric coefficients given as

$$a_0 = 1$$
$$a_k = \frac{(1-m_{i,d})(2-m_{i,d})...(k-m_{i,d})}{(m_{s,i}+1)(m_{s,i}+2)...(m_{s,i}+k)},$$

(A.22)

and where μ_j is defined as

$$\mu_j = \sum_{l=j}^{m_{i,d}-1} a_l \left(\frac{m_{s,i}\bar{\gamma}_{i,d}}{m_{i,d}\bar{\gamma}_{s,i}}\right)^l (-1)^l \binom{l}{j} \quad , j \geq 0$$
$$\mu_j = 0 \qquad\qquad\qquad\qquad\qquad , j < 0 \qquad \text{(A.23)}$$

Similar simplifications can be performed with the second hypergeometric function in (A.19). It can be written as

$$
\begin{aligned}
{}_2F_1\left(1, m_{s,i} + m_{i,d}; m_{i,d} + 1; \frac{m_{i,d}/\bar{\gamma}_{i,d}+s}{m_{s,i}/\bar{\gamma}_{s,i}+m_{i,d}/\bar{\gamma}_{i,d}+s}\right) = \\
\left[\frac{m_{s,i}/\bar{\gamma}_{s,i}+m_{i,d}/\bar{\gamma}_{i,d}+s}{m_{s,i}/\bar{\gamma}_{s,i}}\right] {}_2F_1\left(1, 1-m_{s,i}, m_{i,d}+1; -\frac{m_{i,d}/\bar{\gamma}_{i,d}+s}{m_{s,i}/\bar{\gamma}_{s,i}}\right),
\end{aligned} \tag{A.24}
$$

where

$$
\begin{aligned}
{}_2F_1\left(1, 1-m_{s,i}; m_{i,d}+1; -\frac{m_{i,d}/\bar{\gamma}_{i,d}+s}{m_{s,i}/\bar{\gamma}_{s,i}}\right) &= \sum_{k=0}^{m_{s,i}-1} c_k(-1)^k \left(\frac{m_{i,d}/\bar{\gamma}_{i,d}+s}{m_{s,i}/\bar{\gamma}_{s,i}}\right)^k \\
&= \sum_{k=0}^{m_{s,i}-1} c_k(-1)^k \left(\frac{m_{i,d}\bar{\gamma}_{s,i}}{m_{s,i}\bar{\gamma}_{i,d}}\right)^k \\
&\qquad \times \left(1+\frac{\bar{\gamma}_{i,d}}{m_{i,d}}s\right)^k \\
&= \sum_{j=0}^{m_{s,i}-1} \nu_j \left(\frac{\bar{\gamma}_{i,d}}{m_{i,d}}s\right)^j, \tag{A.25}
\end{aligned}
$$

and c_k are the hypergeometric coefficients give as

$$
\begin{aligned}
c_0 &= 1 \\
c_k &= \frac{(1-m_{s,i})(2-m_{s,i})...(k-m_{s,i})}{(m_{i,d}+1)(m_{i,d}+2)...(m_{i,d}+k)},
\end{aligned} \tag{A.26}
$$

and where ν_j is defined as

$$
\begin{aligned}
\nu_j &= \sum_{l=j}^{m_{s,i}-1} c_l \left(\frac{m_{i,d}\bar{\gamma}_{s,i}}{m_{s,i}\bar{\gamma}_{i,d}}\right)^l (-1)^l \binom{l}{j} \quad , j \geq 0 \\
\nu_j &= 0 \quad\quad\quad\quad\quad\quad\quad\quad\quad\quad\quad\quad , j < 0.
\end{aligned} \tag{A.27}
$$

$$\tag{A.28}$$

By substituting (A.20),(A.21),(A.24),(A.25) back into the MGF of (A.19), we get

$$
M_{\gamma_i}(s) = \left(\frac{m_{s,i}}{\bar{\gamma}_{s,i}}\right)^{m_{s,i}} \left(\frac{m_{i,d}}{\bar{\gamma}_{i,d}}\right)^{m_{i,d}}
$$

$$
\times \frac{\Gamma(m_{s,i}+m_{i,d})}{\Gamma(m_{s,i})\Gamma(m_{i,d})(m_{s,i}/\bar{\gamma}_{s,i}+m_{i,d}/\bar{\gamma}_{i,d}+s)^{m_{s,i}+m_{i,d}}}
$$

$$
\times \left[\frac{1}{m_{s,i}}\left[\frac{m_{s,i}/\bar{\gamma}_{s,i}+m_{i,d}/\bar{\gamma}_{i,d}+s}{m_{i,d}/\bar{\gamma}_{i,d}}\right]\sum_{j=0}^{m_{i,d}-1}\mu_j\left(\frac{\bar{\gamma}_{s,i}}{m_{s,i}}s\right)^{j}\right.
$$

$$
\left.+\frac{1}{m_{i,d}}\left[\frac{m_{s,i}/\bar{\gamma}_{s,i}+m_{i,d}/\bar{\gamma}_{i,d}+s}{m_{s,i}/\bar{\gamma}_{s,i}}\right]\sum_{j=0}^{m_{s,i}-1}\nu_j\left(\frac{\bar{\gamma}_{i,d}}{m_{i,d}}s\right)^{j}\right]
$$

$$
= \frac{D_i}{(m_{s,i}/\bar{\gamma}_{s,i}+m_{i,d}/\bar{\gamma}_{i,d}+s)^{m_{s,i}+m_{i,d}}}\left[(\alpha_{1i}+\beta_{1i}s)\sum_{j=0}^{m_{i,d}-1}\mu_j\left(\frac{\bar{\gamma}_{s,i}}{m_{s,i}}s\right)^{j}\right.
$$

$$
\left.+(\alpha_{2i}+\beta_{2i}s)\sum_{j=0}^{m_{s,i}-1}\nu_j\left(\frac{\bar{\gamma}_{i,d}}{m_{i,d}}s\right)^{j}\right],
$$

(A.29)

where

$$
D_i = \left(\frac{m_{s,i}}{\bar{\gamma}_{s,i}}\right)^{m_{s,i}}\left(\frac{m_{i,d}}{\bar{\gamma}_{i,d}}\right)^{m_{i,d}}\frac{\Gamma(m_{s,i}+m_{i,d})}{\Gamma(m_{s,i})\Gamma(m_{i,d})}
$$

(A.30)

and

$$
\begin{array}{ll}
\alpha_{1i} = \frac{\bar{\gamma}_{i,d}}{\bar{\gamma}_{s,i}m_{i,d}}+\frac{1}{m_{s,i}} & \beta_{1i} = \frac{\bar{\gamma}_{i,d}}{m_{s,i}m_{i,d}}\\
\alpha_{2i} = \frac{\bar{\gamma}_{s,i}}{\bar{\gamma}_{i,d}m_{s,i}}+\frac{1}{m_{i,d}} & \beta_{2i} = \frac{\bar{\gamma}_{s,i}}{m_{s,i}m_{i,d}}
\end{array}
$$

(A.31)

Using [66, 0.316], we see that

$$
(a_0+a_1x)\sum_{k=0}^{n}b_kx^k = \sum_{k=0}^{n+1}(a_0\,b_k+a_1\,b_{k-1})x^k.
$$

(A.32)

Hence, (A.29) can be re-written as

$$
M_{\gamma_i}(s) = \frac{D_i}{(m_{s,i}/\bar{\gamma}_{s,i}+m_{i,d}/\bar{\gamma}_{i,d}+s)^{m_{s,i}+m_{i,d}}}
$$

$$
\times\left[\sum_{j=0}^{m_{i,d}}\left\{(\alpha_{1i}\mu_j\left(\frac{\bar{\gamma}_{s,i}}{m_{s,i}}\right)^{j}+\beta_{1i}\mu_{j-1}\left(\frac{\bar{\gamma}_{s,i}}{m_{s,i}}\right)^{j-1}\right\}s^j\right.
$$

$$
\left.+\sum_{j=0}^{m_{s,i}}\left\{\alpha_{2i}\nu_j\left(\frac{\bar{\gamma}_{i,d}}{m_{i,d}}\right)^{j}+\beta_{2i}\nu_{j-1}\left(\frac{\bar{\gamma}_{i,d}}{m_{i,d}}\right)^{j-1}\right\}s^j\right].
$$

(A.33)

Since $\mu_k = 0$ for all $k > m_{i,d} - 1$, and since $\nu_k = 0$ for all $k > m_{s,i} - 1$,

$$M_{\gamma_i}(s) = \frac{D_i}{(m_{s,i}/\bar{\gamma}_{s,i} + m_{i,d}/\bar{\gamma}_{i,d} + s)^{m_{s,i}+m_{i,d}}}$$
$$\times \left[\sum_{k=0}^{M_i} \left\{ \alpha_{1i}\mu_k \left(\frac{\bar{\gamma}_{s,i}}{m_{s,i}} \right)^k + \beta_{1i}\mu_{k-1} \left(\frac{\bar{\gamma}_{s,i}}{m_{s,i}} \right)^{k-1} \right. \right.$$
$$\left. \left. + \alpha_{2i}\nu_k \left(\frac{\bar{\gamma}_{i,d}}{m_{i,d}} \right)^k + \beta_{2i}\nu_{k-1} \left(\frac{\bar{\gamma}_{i,d}}{m_{i,d}} \right)^{k-1} \right\} s^k \right]. \quad \text{(A.34)}$$

where $M_i = \max(m_{s,i}, m_{i,d})$. Finally, the MGF of the i-th path relay is

$$M_{\gamma_i}(s) = \frac{D_i}{(m_{s,i}/\bar{\gamma}_{s,i} + m_{i,d}/\bar{\gamma}_{i,d} + s)^{m_{s,i}+m_{i,d}}} \left[\sum_{k=0}^{M_i} A_{ik}s^k \right], \quad \text{(A.35)}$$

where

$$A_{ik} = \alpha_{1i}\mu_k \left(\frac{\bar{\gamma}_{s,i}}{m_{s,i}} \right)^k + \beta_{1i}\mu_{k-1} \left(\frac{\bar{\gamma}_{s,i}}{m_{s,i}} \right)^{k-1} + \alpha_{2i}\nu_k \left(\frac{\bar{\gamma}_{i,d}}{m_{i,d}} \right)^k + \beta_{2i}\nu_{k-1} \left(\frac{\bar{\gamma}_{i,d}}{m_{i,d}} \right)^{k-1}. \quad \text{(A.36)}$$

By using (A.1), the total MGF of the network is

$$M_{\gamma_{ub}}(s) = \left(1 + \frac{\bar{\gamma}_{s,d}}{m_{s,d}}s \right)^{-m_{s,d}} \prod_{i=1}^{N} \left(\frac{m_{s,i}}{\bar{\gamma}_{s,i}} + \frac{m_{i,d}}{\bar{\gamma}_{i,d}} + s \right)^{-(m_{s,i}+m_{i,d})}$$
$$\times \prod_{i=1}^{N} \left[D_i \sum_{k=0}^{M_i} A_{ik}s^k \right]$$
$$= \left(1 + \frac{\bar{\gamma}_{s,d}}{m_{s,d}}s \right)^{-m_{s,d}} \prod_{i=1}^{N} \left(\frac{m_{s,i}}{\bar{\gamma}_{s,i}} + \frac{m_{i,d}}{\bar{\gamma}_{i,d}} + s \right)^{-(m_{s,i}+m_{i,d})}$$
$$\times \left[\prod_{i=1}^{N} D_i \right] \left[\sum_{j=0}^{M} B_j s^j \right], \quad \text{(A.37)}$$

where $M = \sum_{i=1}^{N} M_i$ and from [66, 0.316]

$$B_j = \sum_{k=0}^{j} \sum_{l=0}^{k} \sum_{m=0}^{l} \cdots \sum_{q=0}^{p} \sum_{r=0}^{q} \sum_{s=0}^{t} A_{1s} A_{2(r-s)} A_{3(q-r)} \cdots A_{(N-2)(l-m)} A_{(N-1)(k-l)} A_{N(j-k)}. \quad \text{(A.38)}$$

By using partial fractions, (A.37) can be rewritten as

$$M_{\gamma_{ub}}(s) = \left[\prod_{i=1}^{N} D_i \right] \left[\sum_{r=1}^{m_{s,d}} \Delta_r (1 + \frac{\bar{\gamma}_{s,d}}{m_{s,d}}s)^{-r} \right. \quad \text{(A.39)}$$
$$\left. + \sum_{i=1}^{N} \sum_{t=1}^{m_{s,i}+m_{i,d}} \Psi_{ti}(m_{s,i}/\bar{\gamma}_{s,i} + m_{i,d}/\bar{\gamma}_{i,d} + s)^{-t} \right],$$

where

$$\Delta_r = \frac{(\frac{\bar{\gamma}_{s,d}}{m_{s,d}})^{(r-m_{s,d})}}{(m_{s,d}-r)!} \frac{\partial^{m_{s,d}-r}}{\partial s^{m_{s,d}-r}} \left[\sum_{j=0}^{M} B_j s^j \prod_{i=1}^{N} \left(\frac{m_{s,i}}{\bar{\gamma}_{s,i}} + \frac{m_{i,d}}{\bar{\gamma}_{i,d}} + s \right)^{-(m_{s,i}+m_{i,d})} \right]_{s=-m_{s,d}/\bar{\gamma}_{s,d}}$$

(A.40)

and

$$\Psi_{ti} = \frac{(\frac{\bar{\gamma}_{s,i}\bar{\gamma}_{i,d}}{m_{s,i}\bar{\gamma}_{i,d}+m_{i,d}\bar{\gamma}_{s,i}})^t}{(m_{s,i}+m_{i,d}-t)!} \frac{\partial^{m_{s,i}+m_{i,d}-t}}{\partial s^{m_{s,i}+m_{i,d}-t}} \left[\sum_{j=0}^{M} B_j s^j \left[1 + \frac{\bar{\gamma}_{s,d}}{m_{s,d}} s \right]^{-m_{s,d}} \right.$$ (A.41)

$$\left. \times \prod_{k=1,k\neq i}^{N} \left(\frac{m_{s,k}}{\bar{\gamma}_{s,k}} + \frac{m_{k,d}}{\bar{\gamma}_{k,d}} + s \right)^{-(m_{s,k}+m_{k,d})} \right]_{s=-\frac{m_{s,i}\bar{\gamma}_{i,d}+m_{i,d}\bar{\gamma}_{s,i}}{\bar{\gamma}_{s,i}\bar{\gamma}_{i,d}}}.$$

By taking the inverse Laplace transform of $M_{\gamma_{ub}}(s)$ in (A.39) and using the fact that $\mathcal{L}^{-1}\{(1+as)^{-k}\} = \frac{1}{(k-1)!a^k} x^{k-1} e^{-\frac{x}{a}}$, the PDF of γ_{ub} is calculated as follows:

$$f_{\gamma_{ub}}(\gamma) = \left[\prod_{i=1}^{N} D_i \right] \left[\sum_{r=1}^{m_{s,d}} \frac{\Delta_r}{(r-1)!} \left(\frac{m_{s,d}}{\bar{\gamma}_{s,d}} \right)^r \gamma^{r-1} e^{\frac{-\gamma m_{s,d}}{\bar{\gamma}_{s,d}}} \right.$$ (A.42)

$$\left. + \sum_{i=1}^{N} \sum_{t=1}^{m_{s,i}+m_{i,d}} \frac{\Psi_{ti}}{(t-1)!} \left(\frac{m_{s,i}\bar{\gamma}_{i,d}+m_{i,d}\bar{\gamma}_{s,i}}{\bar{\gamma}_{s,i}\bar{\gamma}_{i,d}} \right)^t \gamma^{t-1} e^{-\gamma \frac{m_{s,i}\bar{\gamma}_{i,d}+m_{i,d}\bar{\gamma}_{s,i}}{\bar{\gamma}_{s,i}\bar{\gamma}_{i,d}}} \right].$$

Appendix B

PDF of the approximation for received SNR under C-MRC scheme

By substituting s by $0.5\,s$ in (A.7), the MGF of $0.5\min(\gamma_{s,i}, \gamma_{i,d})$ can be derived. Therefore, the MGF of the total received SNR given in (4.6) can be written as

$$M_{\gamma_{\text{tot}}}(s) = M_{\gamma_{s,d}}(s) \prod_{i=1}^{N} M_{\gamma_i}(0.5\,s)\,. \tag{B.1}$$

Since $\gamma_{s,d}$ is Gamma-distributed with shape parameter m and scale parameter $\bar{\gamma}/m$, $M_{\gamma_{s,d}}(s)$ can be written as (A.2). Therefore, by using (A.7) and (A.2) with (B.1), we get

$$
M_{\gamma_{\text{tot}}}(s) = \left[1 + \frac{\bar{\gamma}}{m}s\right]^{-m} \left[\left(\frac{m}{\bar{\gamma}}\right)^{2m-1} \frac{\Gamma(2m)}{m\Gamma^2(m)}\right.
$$
$$
\left. \times \frac{2}{(2m/\bar{\gamma} + 0.5\,s)^{2m-1}} \sum_{k=0}^{m-1} a_k \left(-\frac{m/\bar{\gamma} + 0.5\,s}{m/\bar{\gamma}}\right)^k\right]^N. \tag{B.2}
$$

By performing further simplifications similar to those of (A.8) to (A.14), we arrive at

$$M_{\gamma_{\text{tot}}}(s) = \frac{\Gamma^N(2m)(0.5)^{2N(m-1)}}{m^N\Gamma^{2N}(m)\left[1 + \frac{\bar{\gamma}}{m}s\right]^m \left[1 + \frac{\bar{\gamma}}{4m}s\right]^{N(2m-1)}} \sum_{j=0}^{N(m-1)} \lambda_j \left(\frac{\bar{\gamma}}{2m}s\right)^j, \tag{B.3}$$

where $\lambda_j = \frac{1}{j\delta_0}\sum_{r=1}^{j}(rN - j + r)\delta_r\lambda_{j-r}$ with $\lambda_0 = \delta_0^N$ and δ_j is defined as $\delta_j = \sum_{i=j}^{m-1} a_i(-1)^i \binom{i}{j}$. By using partial fractions, (B.3) can be rewritten as

$$M_{\gamma_{\text{tot}}}(s) = \frac{\Gamma^N(2m)}{2^{2N(m-1)}m^N\Gamma^{2N}(m)} \left[\sum_{r=1}^{m}\Lambda_r\left(1 + \frac{\bar{\gamma}}{m}s\right)^{-r} + \sum_{t=1}^{N(2m-1)}\Omega_t\left(1 + \frac{\bar{\gamma}}{4m}s\right)^{-t}\right],$$
$$\tag{B.4}$$

where

$$\Lambda_r = \frac{\left(\frac{\bar{\gamma}}{m}\right)^{(r-m)}}{(m-r)!} \frac{\partial^{m-r}}{\partial s^{m-r}} \left[\sum_{j=0}^{N(m-1)} \lambda_j \left(\frac{\bar{\gamma}}{2m}s\right)^j \left(1 + \frac{\bar{\gamma}}{4m}s\right)^{-N(2m-1)} \right]_{s=-m/\bar{\gamma}} \tag{B.5}$$

and

$$\Omega_t = \frac{\left(\frac{\bar{\gamma}}{4m}\right)^{(t-N(2m-1))}}{(N(2m-1)-t)!} \frac{\partial^{N(2m-1)-t}}{\partial s^{N(2m-1)-t}} \left[\sum_{j=0}^{N(m-1)} \lambda_j \left(\frac{\bar{\gamma}}{2m}s\right)^j \left(1 + \frac{\bar{\gamma}}{m}s\right)^{-m} \right]_{s=-4m/\bar{\gamma}} . \tag{B.6}$$

By taking the inverse Laplace transform of $M_{\gamma_{\text{tot}}}(s)$ in (B.4) and using the fact that $\mathcal{L}^{-1}\{(1+as)^{-k}\} = \frac{1}{(k-1)!a^k}x^{k-1}e^{-\frac{x}{a}}$, the PDF of γ_{tot} is calculated as follows:

$$\begin{aligned}
f_{\gamma_{\text{tot}}}(\gamma) &= \frac{\Gamma^N(2m)}{2^{2N(m-1)}\, m^N\, \Gamma^{2N}(m)} \left[\sum_{r=1}^{m} \frac{\Lambda_r}{(r-1)!} \left(\frac{m}{\bar{\gamma}}\right)^r \gamma^{r-1} e^{\frac{-\gamma m}{\bar{\gamma}}} \right. \\
&\quad + \left. \sum_{t=1}^{N(2m-1)} \frac{\Omega_t}{(t-1)!} \left(\frac{4m}{\bar{\gamma}}\right)^t \gamma^{t-1} e^{\frac{-\gamma 4m}{\bar{\gamma}}} \right]. \tag{B.7}
\end{aligned}$$